UCRL-8377
Particle Accelerators
and High-Voltage Machines

UNIVERSITY OF CALIFORNIA

Radiation Laboratory
Berkeley, California

Contract No. W-7405-eng-48

THE STRAY RADIATION FIELD OF THE BEVATRON

Alan R. Smith

July 16, 1958

Printed for the U. S. Atomic Energy Commission

DISCLAIMER

THE STRAY RADIATION FIELD OF THE BEVATRON

Alan R. Smith

Radiation Laboratory
University of California
Berkeley, California

July 16, 1958

ABSTRACT

Radiation survey work at the Berkeley Bevatron has been a continuous project of the Health Physics Group since start-up of the accelerator in November, 1954. A substantial body of survey data has accumulated, from which a general pattern for the stray radiation field can be constructed. This report includes a summary of the characteristics of the radiation field pattern as currently understood, a description of the various techniques used to make radiation measurements, and a discussion of some serious problems encountered in survey work at this accelerator.

THE STRAY RADIATION FIELD OF THE BEVATRON

Alan R. Smith

Radiation Laboratory
University of California
Berkeley, California

July 16, 1958

THE BEVATRON: GENERAL DESCRIPTION

A brief description of the Bevatron[1, 2] is given here to serve as an aid in understanding the main body of this report. Figure 1 is a plan view of the Bevatron building, showing the main features of the machine, shielding, and surrounding work areas; the drawing is to scale and depicts the current status of these features.

The accelerator consists of a large ring-shaped magnet which completely encloses the vacuum tank with at least 2 ft of iron except at four equally spaced straight sections, called tangent tanks. The mean radius of the proton-beam orbit is 50 ft, and the beam median plane is 8 ft above the level of the floor outside the magnet structure. The main shield, located just outside the magnet, encircles all but a portion of the machine near the injector. The building is roughly circular, except for the motor generator wing, and is 105 ft in radius, with an additional 30 ft radially along the south portion. This outer space at the south on the main floor accommodates various shops, the main control room, and the experimental counting facilities. Directly above these facilities on the Mezzanine, 15 feet above floor level, are offices and some additional shops. An experimental area has been added to the northwest portion of the building subsequent to the work reported here.

The circular building is marked off into 24 equal angular segments, termed bays; this division of space has provided a basis for the physical layout of survey work. The entire area outside the shield and inside the building should be available for continuous occupancy; shielding efforts have always been directed toward this end.

The main shield is 5 ft thick and between 15 and 19 ft high; it is of ordinary concrete except for the middle course (around the median plane) which is of high-density concrete. The shield is augmented at both the south straight section and the west straight section, the principle target areas. No roof shielding has yet been installed over any portions of the machine.

Nearly all important control and experimental facilities are located near or in the four tangent tanks. The east tangent tank (ETT) contains parts of the injection system, one set of beam-measuring electrodes and a heavy plunging beam clipper. The south tangent tank (STT) houses another set of beam-induction electrodes and several plunging probes. The west tangent tank (WTT) area is the main experimental portion of the machine. The tank houses a variety of plunging probes, and nearby in the upstream direction

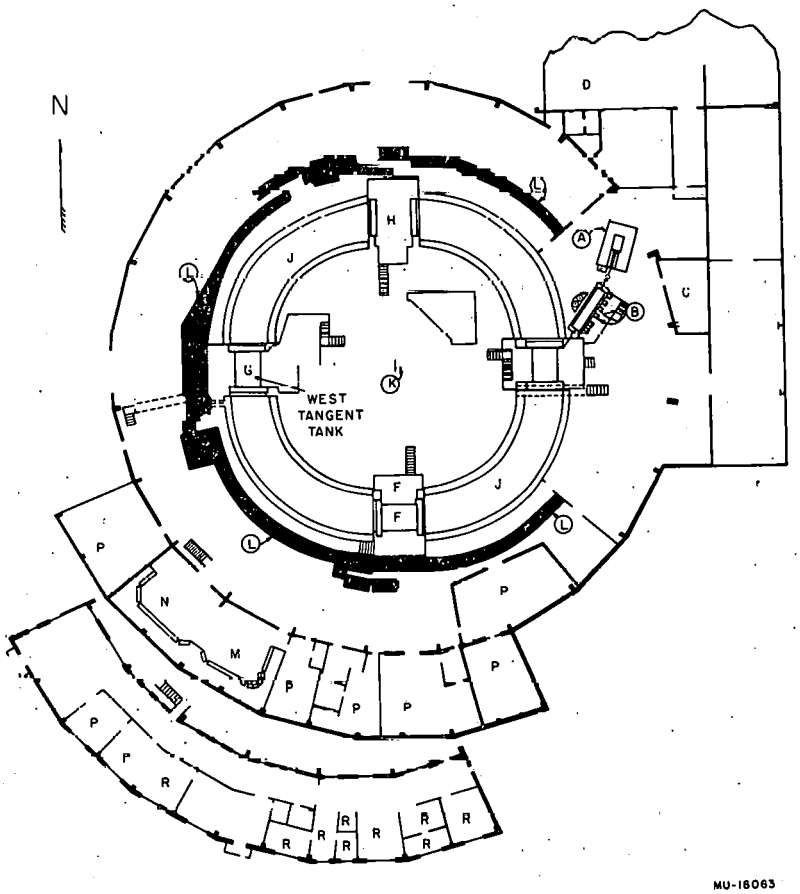

Fig. 1. Plan view of Bevatron showing (A) Cockcroft-Walton accelerator, (B) linear accelerator, (C) injector control room, (D) motor-generator room, (E) east tangent tank, (F) south tangent tank, (G) west tangent tank, (H) north tangent tank, (J) magnet quadrants (4), (K) magnet-pit center, (L) main shield, (M) main control room, (N) experimental counting area, (P) shop facilities, (R) office space, and (1 through 24) bays.

inside the southwest magnet quadrant are located several flip-up probes. The north tangent tank (NTT) contains the beam accelerating electrodes. Any of the probes can carry targets into position for experimental purposes.

An operating cycle of the Bevatron proceeds as follows. A bunch of protons is injected at the ETT from the linear accelerator — Cockcroft-Walton accelerator injector system. After an acceleration period of slightly less than 2 seconds, a substantial fraction (about 10%) of the injected beam reaches an energy of 6.2 Bev. At a predetermined time before the desired beam energy is attained, typically 50 to 100 milliseconds early, the required targets are brought into position either inside or outside the beam orbit. The beam is then driven radially onto the targets by changing control parameters appropriately. At maximum energy a period of 4 sec is required to restore the initial conditions of the machine to receive and accelerate a second bunch of protons; thus cycles recur at a rate of 10 per minute.

A partial list of Bevatron terminology, with definitions, is included here, because these terms are in constant usage in survey work;

(a) Current marker, or I pip: A timing pulse (34 in number) that occurs at a certain magnet current, and thus at a particular beam energy; the high energy I pips and corresponding energies are tabulated as follows:

I number	Energy (Bev)
I-25	3.2
I-26	4.15
I-27	4.8
I-28	5.3
I-29	5.7
I-30	6.1
I-31	6.2

(b) Tangent tank: one of the four straight sections located between magnet quadrants.

(c) Targets: Two classes are in general use:

(1) Plunging targets, actuated pneumatically and located in tangent tanks. Designation of these targets is according to tangent tank, position with respect to the beam, and position in the particular tangent tank. Thus the WIN target is in the west tangent tank, is operated from inside the beam orbit, and is located at the north (downstream) end of this tangent tank.

(2) Flip-up targets, actuated magnetically to rotate 90 degrees into vertical position at the median plane, and located in the magnet quadrants. Designation is according to magnet quadrant and degrees of arc in this quadrant either upstream or downstream from a tangent tank.

RADIATION DETECTORS

General

The various radiation detectors used at the Bevatron include ionization chambers, proportional pulse counters, nuclear-track emulsions, neutron-activated foils, and scintillation counters. Because of the low duty cycle of the accelerator, the only acceptable mode of operation for these detectors is to integrate their response. While this is an inherent property of emulsions and foils, it is not so with the other detectors, which provide instantaneous information that is not naturally stored for a long enough time. Thus the charge collected by an ion chamber must be stored and subsequently measured; pulses from the other counters must be counted and recorded by scaling circuitry.

The practical consequence of this situation is our almost complete reliance on standard UCRL rack-mounted electronic counting equipment for survey work. Portable battery-operated radiation-detection instruments have seldom been used, with exceptions as noted in the following paragraphs of this section.

Ionization Chambers

The ionization chambers used are thin-walled plastic chambers filled with atmospheric air, with their inner surfaces made conductive by a thin layer of Aquadag. Such simply constructed chambers have been found to exhibit response that closely follows the response of a "tissue-equivalent chamber" in radiation fields of the constitution found here. Positive ions are collected at the center electrode which is coupled to either of two indication instruments. Two different size ion chambers are used, a large chamber of 5200 cm^3 volume, and a small chamber of 200 cm^3 volume. Photographs of both instruments with the two ion chambers are shown in Figs. 2 and 3.

The indicating instruments must be extremely sensitive, and very carefully constructed to minimize leakage of chamber charge, because the ionizing radiation levels are often less than 1 microroentgen (μr) per 10^{10} accelerated protons. The more sensitive and more reliable of the two instruments is a Lindemann integrating electrometer which is easily capable of detecting 0.03 μr per Bevatron pulse when used with the large ion chamber. (The limitation here is a result of the natural background radiation level, which is of the order of 0.02 - 0.03 μr per 6 seconds - the duration of the Bevatron cycle.) The instrument is basically a quartz-fiber electrometer which has continuously variable sensitivity via adjustment of the quadrant voltages. Calibration of the instrument with each ion chamber is performed in a known field of radium gamma rays at every instrument sensitivity used in actual survey work. The Lindemann electrometer serves as a standard for low-level measurements of ionizing radiation; however, it is an awkward device to carry about and can be read only by observation through a microscope.

Thus a second and more truly portable integrating electrometer has been built. This unit utilizes a two-tube electronic circuit with a self-contained

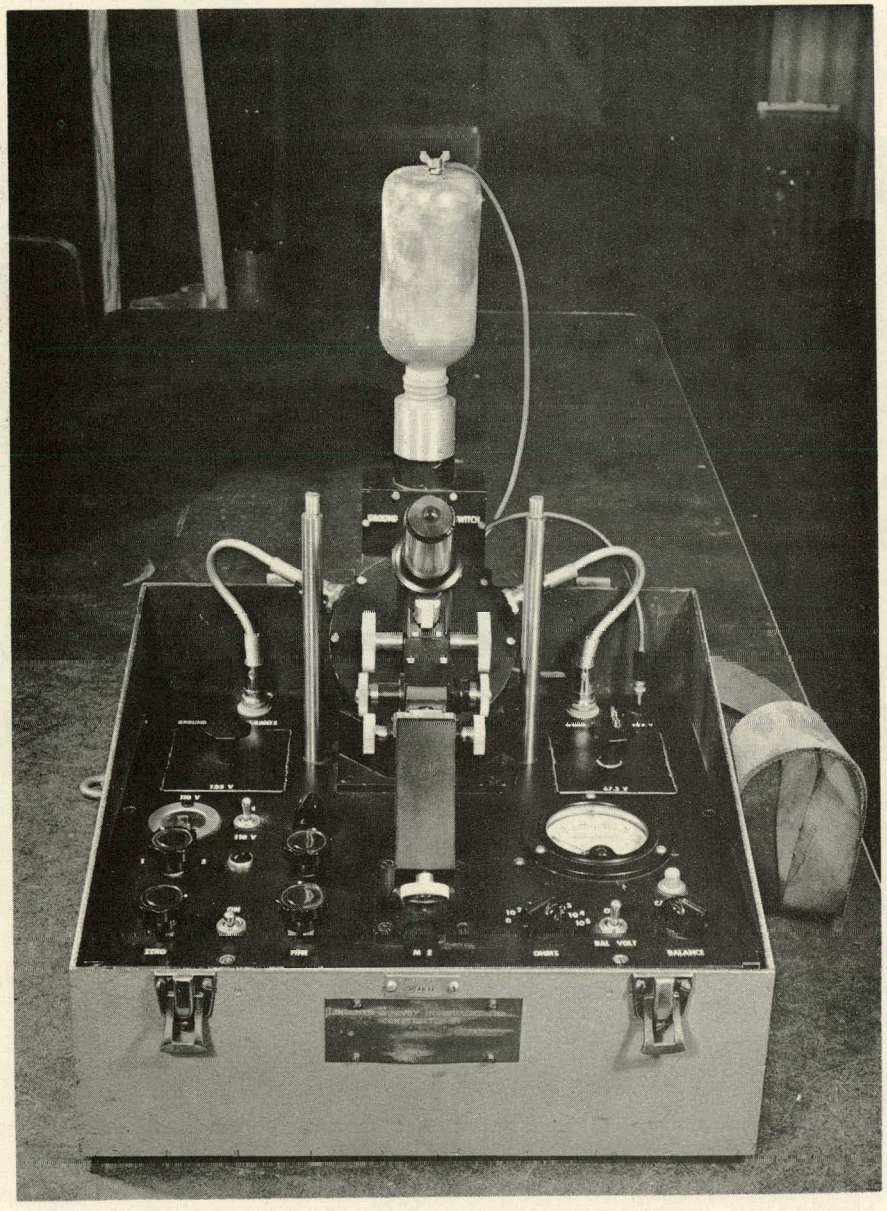

ZN-2046

Fig. 2. Lindemann electrometer with small ion chamber.

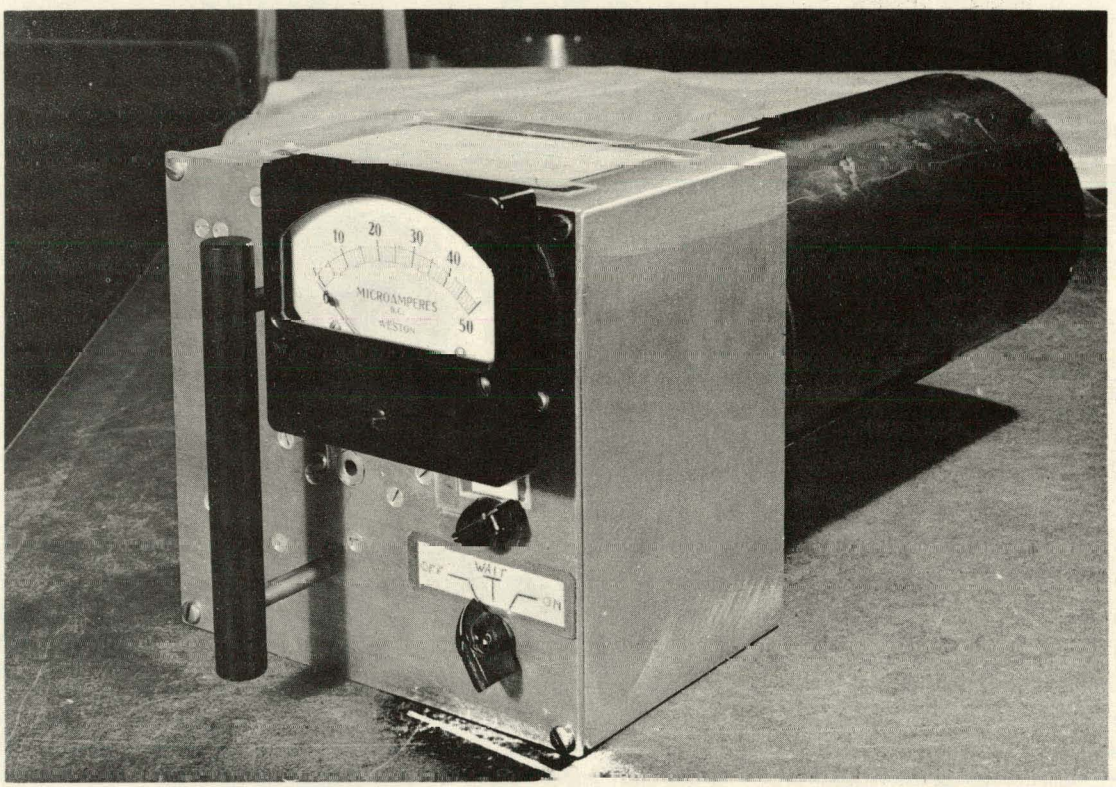

ZN-2043

Fig. 3. Portable integrating electrometer with large ion chamber.

battery supply. The integrated charge is read as a current on a 50 μamp full-scale microammeter of the core-magnet type. The instrument is calibrated in a known flux of radium gamma rays with the same two ion chambers. Sensitivity can be adjusted over a range of 7:1 for each chamber by changing the capacitance of the variable air capacitor which stores the charge collected on the ion chamber electrode. In normal practice, the instrument operates near maximum sensitivity; typical sensitivity values are: 150 μr per full scale with the small ion chamber, and 10 μr per full scale with the large ion chamber. Most work in occupied areas at the Bevatron requires maximum sensitivity with the large chamber, in which case a beam pulse producing 0.2 μr at the chamber will cause an upscale deflection of one division on the indicating meter. At these same instrument conditions, the background-radiation level causes an upscale deflection of from 1 to 2 divisions per minute. (This is a measured background level of 0.012 to 0.024 milliroentgens/hour which compares well with a typical Lindemann measurement of 0.017 mr/hr for background level.)

Performance of the portable integrator has been carefully checked against that of the Lindemann Electrometer under Bevatron operating conditions - strong pulsed magnetic fields, strong radiofrequency-energy fields, large electrical noise transients. Performance has been found satisfactory everywhere except in an area within a few feet of the linear-accelerator oscillators. This instrument has been used extensively for ionizing-radiation surveys around the Bevatron.

Proportional Counters

The most widely used radiation detectors are proportional counters, and these are employed primarily to count neutrons. Two kinds of proportional counters have been used; one is sensitive to slow neutrons, the other is sensitive to fast neutrons; both are relatively insensitive to gamma rays. Photographs of the counters and a cathode-follower coupling unit are shown in Fig. 4.

Slow neutrons are detected by the (n, α) reaction in a brass-wall BF_3-gas counter. The BF_3 gas is enriched in the B^{10} isotope to 96% $B^{10}F_3$. Standard gas filling pressure is 20 cm Hg absolute, although lower gas pressures have been used for reduced sensitivity counters. A standard counter of 25 cm length and 4 cm diameter operates at a high voltage in the neighborhood of 2000 volts, with a useful plateau of 300 to 400 volts. Counter pulses are amplified so that most (n, α) events produce pulse heights of 50 to 100 volts, while pulses from gamma events are no greater than 5 volts; the counter provides excellent discrimination against competing events.

Calibration of slow-neutron counters is performed in the known thermal flux generated by a Po–Be neutron source placed with the counters in a cubical concrete enclosure. A counter filled to 20-cm Hg pressure produces ~4 counts/sec in a 1 neutron/cm^2-sec. thermal flux of the calibration facility.

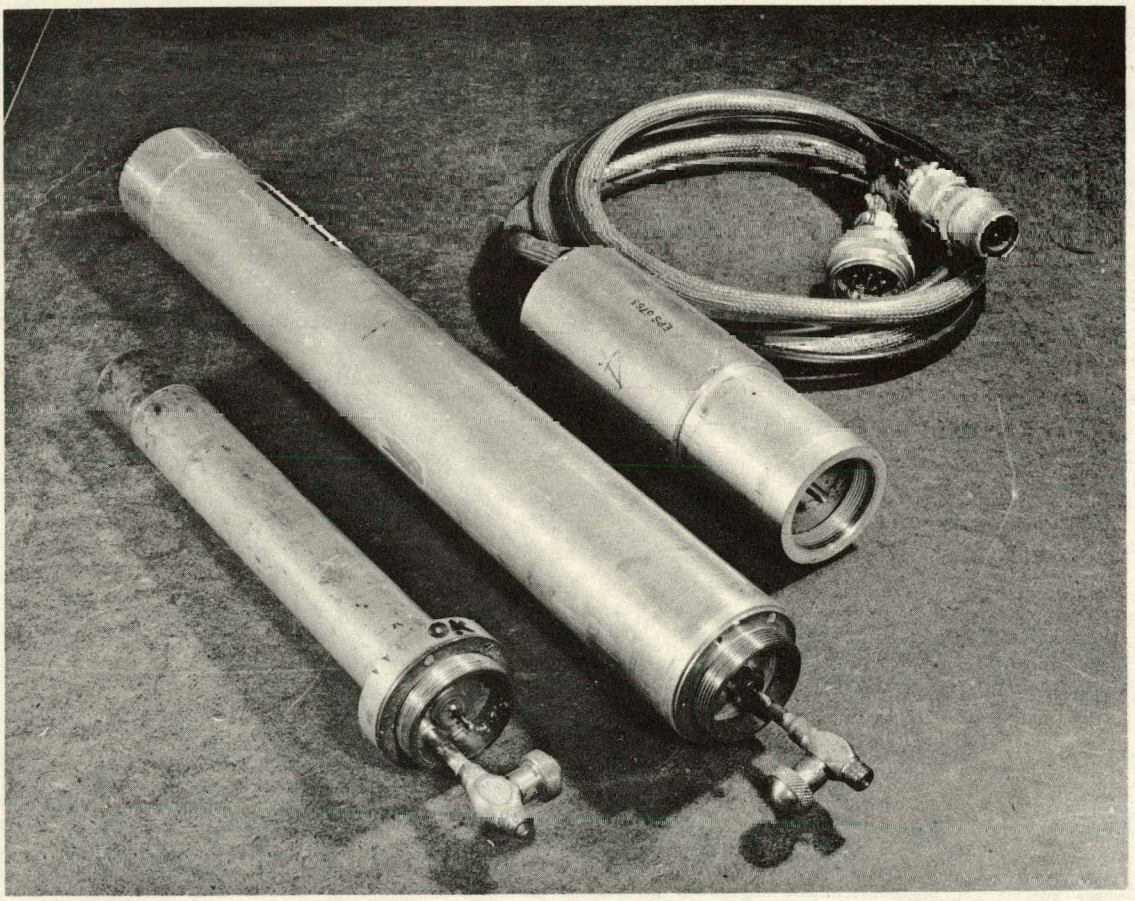

ZN-2044

Fig. 4. Standard BF_3-filled proportional counter, standard PE-lined proportional counter, and cathode-follower coupling unit.

One means of detection of fast neutrons is also accomplished with the BF_3 counter; the counter in this case must be surrounded by an appropriate thickness of moderator. (Paraffin is commonly used as a moderating material.) Either of two moderator configurations has been employed: (a) a Hanson-McKibben Counter[3, 4] or (b) a series of paraffin jackets of various thicknesses that (almost) completely surround the counter. Both systems have relatively high efficiency and are capable of producing 2 to 4 counts/sec. in a fast neutron flux of 1 n/cm^2-sec when used with a 20 cm pressure BF_3 counter. A discussion of the properties of these counting systems appears in the section dealing with neutron-energy determination.

The standard detector of fast neutrons is the polyethylene-lined proportional counter 40 cm in length and 6 cm in diameter. The polyethylene liner is generally chosen to be 1/8-inch thick, and the counter is normally filled to 76 cm Hg pressure with an Argon - 5% CO_2 mixture. Response of this type counter may be shown to be proportional to the product Energy $\times$ Flux Density.[5] The constant of proportionality for the particular counters here employed is 15 mev/cm^2 per count for a fast-neutron flux normal to the counter axis. With a 1/8-inch thick liner the energy–flux density relationship holds up to the vicinity of 20 Mev neutron energy. Competition of gamma events limits the minimum energy response to ~0.2 Mev neutron energy unless extreme care is taken in operational procedure. Thus the practical useful range for the counter is 0.2 to 20 Mev neutron energy.

It is important to note that the constant 15 Mev/cm^2 per count refers to the zero intercept of an integral bias curve taken with the counter. The zero bias intercept is always an extrapolated point, and care must be taken when performing this extrapolation. In addition, there is no clean separation between neutron events (proton recoils) and gamma events, as with the BF_3 counter. This requires careful selection of the counter operating region to insure that gamma events are not taken to be neutron events.

A typical polyethylene-lined counter filled to 76 cm Hg pressure operates at 1800 to 1900 volts. The amplified counter pulses range up to 100 volts when the counter is exposed to a Po–Be neutron source. A radium gamma field of 1 to 2 r/hr would then produce pulses up to 20 to 25 volts in amplitude. The operating point for the scaler discriminator might reasonably be chosen as 30 volts, at which point the observed count rate from the Po Be source is roughly 60% of the extrapolated zero-bias count rate.

Calibration and set-up of the counter thus consists of determination of an integral bias curve in a known flux of Po–Be neutrons, determination of the end point for the radium gamma events from a flux at least as intense as the gamma flux expected at survey locations, and selection of a discriminator setting above this end point. The integral bias curve generated with a Po–Be source shows counter response in an essentially gamma-free fast-neutron flux, and shows the conversion factor that must be applied to counter data obtained with the chosen discriminator level to reduce survey measurements to units of Mev/cm^2. Behavior of the counter in a appropriately intense radium gamma field enables one to select a discriminator setting high enough to exclude the gamma events, but at the same time low enough to permit registry of a large fraction (50 to 70%) of fast-neutron events.

The instantaneous gamma-flux levels encountered at the Bevatron can be surprisingly high. For example, a typical survey location on the main floor shows 5 μr per machine pulse measured with the ion-chamber instruments. At least 90% of this total radiation accompanies beam spillout at the end of the accelerating cycle, a time interval of between 10 and 100 milliseconds. The equivalent steady-state radiation levels range from 1800 to 18000 mr/hr for these spillout conditions. The higher of these intensities generates an environment in which operation of the counters must be checked very carefully to insure that only neutrons are counted, because the numerous gamma events can "pile up" to produce pulse heights considerably greater than any single pulse.

A third type of pulse counter has seen extensive use at the Bevatron—a pulse ion chamber. This chamber detects the fission of U^{235} by slow neutrons; it is fully described in the Radiation Monitor section.

Neutron-Sensitive Emulsions, Foil Activation

The uses of nuclear-track emulsions and neutron-activated foils are described in the sections dealing with results obtained, pages 58 - 60 and pages 60-70 respectively.

Scintillation Counters

Scintillation counting has been employed only rarely, and then not in a quantitative manner. Severe magnetic shielding problems accompany the use of phototubes near the Bevatron, and the solution to these problems is at the expense of mobility. Of greater importance is the fact that for the energy range 0.2 to 20 Mev, no neutron-sensitive scintillators are available that resolve neutron events in the presence of gamma events to the degree required in survey work. As greater emphasis is placed on work with threshold detectors, scintillation counting techniques will undoubtedly come into more extensive use.

Electronic Equipment

The proportional counters are used with standard UCRL rack-mounted electronics equipment. Counter high voltage is supplied from an electronically regulated high voltage source, and is metered with an electrostatic voltmeter. Counters are coupled mechanically to cathode-follower units of 125-Ω output impedance; the low output impedance permits use of at least 200 feet of cable between counter and rack equipment. Signals from the cathode follower drive a linear pulse amplifier that produces positive output pulses up to 100 volts in height at a low impedance level. Amplifier voltage gains of between 6000 and 10,000 are commonly used with a frequency bandpass of 2 megacycles. The pulses are counted on either a binary or decade scaler which is driven by a high-stability pulse-height discriminator. Figure 5 is a photograph of a survey rack containing all the electronic equipment needed to run two counters, complete with a forced-air cooling system, wheels, and lifting eyes; a portable oscilloscope can be carried on the shelf at the left side of the rack.

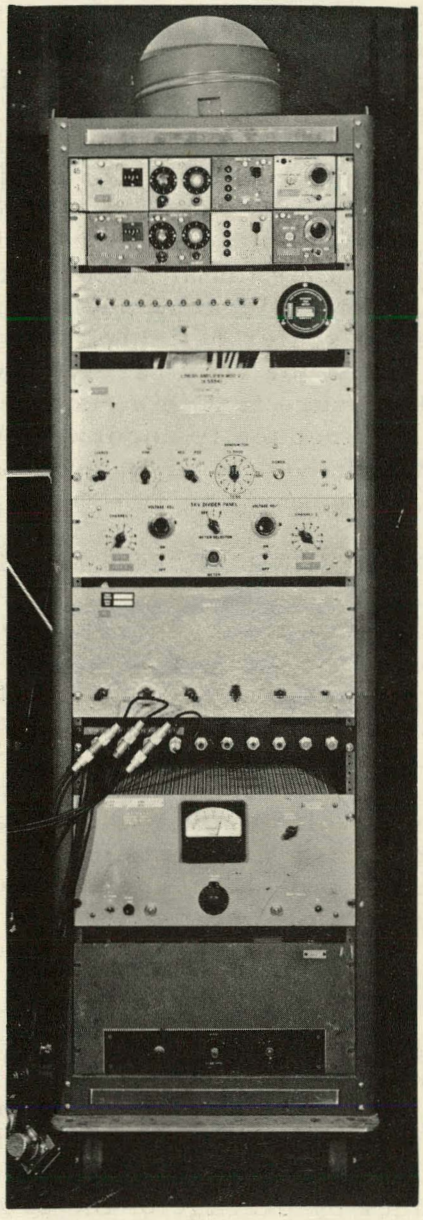

ZN-2045

Fig. 5. Complete survey rack, containing all the equipment required to run two proportional counters.

Counter performance is continually monitored with an oscilloscope during survey work, as a matter of course. Such visual observation of the amplifier pulse output can show immediately the presence of many troubles that might otherwise be difficult or impossible to detect. The problems of electrical and magnetic noise interference are generally evaluated and resolved via the oscilloscope. A whole spectrum of troubles which show up as deteriorating pulse shape are easily seen on the scope; these troubles often develop gradually and may be very hard to notice in scaler data but can at the same time render this data virtually worthless.

Certainly one of the most useful oscilloscope functions is its ability to show quickly and simply whether instantaneous counting rates are too high for the electronic circuitry. Because pulse pairs must be separated by at least 5 μsec to drive the scaler reliably, it is only necessary to determine that two pulses never (or very rarely) occur within this time interval on a scope trace to assure that this requirement is met. High instantaneous count rates are frequently encountered, and this technique of oscilloscope observation has proved to be an invaluable aid to successful survey work.

BEVATRON RADIATION MONITOR

Because the stray radiation field generated by a particle accelerator is incidental to the purpose of the machine, neither operators nor experimenters direct much effort to maintain constancy of this extraneous flux. Whenever possible, effort is channeled to reduce the stray flux to a minimum, but not usually to a constant minimum. Significant variations can be expected, and must be taken into account when survey results are analyzed; this is of particular importance if the over-all radiation pattern is to be constructed from the various measurements. At the Bevatron this variation is sometimes so significant that it has rendered interpretation of data all but impossible. Certainly, one of the greatest difficulties with Bevatron survey work has been the problem of correlating measurements taken at different locations and/or different times.

For this reason, a great deal of attention and much effort has been devoted to the development of facilities designed to furnish the information needed to permit reliable correlation of survey measurements. The Bevatron supplies some of this information. The proton beam is continuously "observed" by means of a system of induction electrodes. The signal generated on these electrodes by passage of the proton beam through their hollow structure is amplified to a suitable level and then presented in various ways as beam information. Both beam magnitude and radial beam position, in particular, can be ascertained from this information.

Accelerator operators normally observe the beam as a dual-rf, envelope on a slow-sweep oscilloscope; the relative amplitudes of these two envelopes indicates the radial position of the beam orbit, while the sum of the envelopes is proportional to the total circulating proton beam at each instant. The sum signal is often presented as a single envelope on a second scope. (There are other types of beam-information display, but these are not generally useful in radiation-survey work.)

The sum signal, proportional to the proton beam, becomes a quantitative measure of the beam magnitude when the proper calibration is applied. This signal is generally used to indicate proton-beam magnitude by operators and experimenters; it has also always provided useful information for radiation-survey measurements.

The sum signal is also presented on an integrating chart recorder--a system designed to indicate the total number of accelerated protons. Included in this system is a tuned rf amplifier and switching relays which permit the integrator to "see" the beam magnitude at only one predetermined instant. The instant is chosen typically close to maximum beam energy, and it is inferred that the beam of this magnitude reaches maximum energy; such may not be the case. In a similar manner, the integrator tells nothing of beam loss prior to its sampling time. These two possible sources of inaccuracy (of which the latter is the more serious), plus the difficulties experienced in attempting to maintain calibration of the equipment, have combined to render the system an often unreliable monitor for our purposes.

Two encouraging factors should be noted, however, both should enhance the value of the induction-electrode integrator information to survey work: (a) the Bevatron has steadily become a more stable and reliable accelerator; (b) recent engineering modifications to the entire induction-electrode system should greatly improve its reliability. The improvements in Bevatron performance tend to reduce beam loss prior to maximum energy, while improvements in the system itself render its response more believable. There has been no opportunity to check these things yet.

Because the Bevatron equipment has not supplied information to satisfy radiation monitoring requirements, it has been necessary to investigate the establishment of separate monitor systems, based on the stray radiation rather than on the primary proton beam.

Numerous attempts have been made to establish a reliable means for correlating data from different survey points and from different times. One such method employes a slow-neutron counter located along the vertical axis of the Bevatron. This counter sees all parts of the machine equally, and should therefore be relatively insensitive to local variations in beam dynamics and target configurations.

Initial investigation of the centrally located monitor was undertaken in October 1955 during a Bevatron run that provided long periods of steady high-intensity beam and essentially constant experimental conditions. The behavior of the monitor, a BF_3 counter (BF_3-13), was compared to the response of two counters located outside the shielding at the rear of Bay 20 – a BF_3 counter (BF_3-16) and a polyethylene-lined counter, (PE-1)--and compared to the total integrated proton beam, as indicated by the induction-electrode beam-monitor system.

Table I is a summary of representative data obtained at this time. The following important facts are evident from the data:

Table I

Radiation monitor data: initial investigation of central pit monitor.

Data Sets	Runs	Target		Beam condition and energy (Bev)	Proton Integrator/ BF_3-13[b]	BF_3-16/ BF_3-13[b]	PE-1/ BF_3-13
		Location	Description				
I	1 through 5	S1W	Chem	5.7	1.28 $^{+.03}_{-.05}$	1.05 $^{+.04}_{-.06}$	3.54
II	9 through 14	2°31' upstream from WTT	Cu	6.2	0.77 $^{+.02}_{-.01}$	0.92 $^{+.03}_{-.04}$	2.99
III	15 through 18	2°31' upstream from WTT	Cu	6.2 [a]steering beam	0.84 $^{+.04}_{-.01}$	1.30 $^{+.13}_{-.08}$	5.68
IV	19 and 20	2°31' upstream from WTT	Cu	6.2 Beam stable	0.77 $^{+0.2}_{-.00}$	0.98 $^{+.01}_{-.00}$	3.76

[a] An attempt was made during these runs to shift the beam orbit slightly to modify the spill-out pattern. The beam would not shift as desired; the conditions for Runs 19 to 20 are, again, these existing for Runs 9 to 14.

[b] ± values show maximum deviations of separate runs in a set from the average value for all runs in a set.

(a) At 6.2 Bev the relative response of the proton integrator to BF_3-13 remains constant for the three sets of Bevatron operating conditions whereas the two Bay-20 counters show wide variations in this respect.

(b) The relative response of the proton integrator to BF_3-13 is sensitive either to beam energy or target position, or both, as shown by comparison of the 6.2 Bev with 5.7 Bev sets.

These points suggest that for given beam energy and target location a meaningful correlation can be established between the proton beam via the beam monitor and the center slow-neutron monitor, and further, that the calibration should hold to within 10% for the duration of this mode of Bevatron operation. Such a comparison can be performed immediately following calibration of the proton-beam monitor, thus insuring the best calibration available. Because the slow neutron counting system is much more stable than the proton-beam monitor system, a monitor of greater reliability for Health Physics purposes should result from this procedure.

Another set of data, shown in Table II, illustrates the sort of problems often encountered in analysis of Bevatron survey data. These runs were also taken during the period of initial experiments with the central monitor. The data was taken during a period when the proton-beam monitor exhibited unstable behavior. Four different calibrations for the monitor were taken, each time comparing integrator response to the control-room oscilloscope.

It can be seen from Table II that for each set of data, the ratio proton integrator/BF_3-13 is constant within 5% of the average for the set, and that these sets represent definite jumps in the response of one of the counters. Because BF_3-13 calibration was known to remain constant, either the slow-neutron flux in the pit, or the proton monitor calibration must have changed. Over-all beam level as read by the Control Room oscilloscope was observed to be reasonably steady at approximately 10^{10} protons per pulse throughout these measurements.

Sets I, II, and III were obtained under identical conditions insofar as the operators could determine. Both BF_3-16 and Pe-1 showed approximately the same relative response for all three sets; but the proton-monitor relative response showed a definite jump for Set III. This abrupt change occurred at the same time that the proton monitor calibration shifted. These facts are taken to mean that the proton-monitor sensitivity changed, and that the radiation field remained essentially constant.

Sets IV and V were obtained under two different beam-steering conditions, each condition different from the initial conditions. Considerable variation in response of all detectors is noted. Data obtained in later work with indium foils (pages 60 - 70) shows that great variations in the radiation intensity can be expected near tangent tanks for different target configurations, and when beam dynamics are changed, as in the above case. In particular, if much of the beam were lost at high energy near the STT, these high readings for the Bay-20 counters would be expected. It is worth noting that for both these sets, the beam was forced to a smaller-radius orbit.

Table II

Radiation monitor data showing erratic behaviour of proton-beam monitor for single target location[a]

Data Sets	Run Nos., Inclusive Runs	Beam condition and energy (Bev)	Proton Integrator/ BF_3-13[b]	BF_3-16/ BF_3-13[b]	PE-1/ BF_3-13	Proton Integrator Calibration 10^{10} p/div.
I	10 to 13	6.2	$1.11^{+.02}_{-.05}$	$1.06^{+.02}_{-.04}$	-	2.1
II	14 to 17	6.2	$1.13^{+.04}_{-.05}$	$1.09^{+.06}_{-.06}$	4.16	2.1
III	18 to 22	6.2	$0.78^{+.04}_{-.02}$	$1.00^{+.06}_{-.04}$	3.71	1.76
IV	25 to 28	6.2 [c] steering beam	$1.02^{+.04}_{-.04}$	$1.46^{+.06}_{-.07}$	7.93	2.56
V	29 to 31	[c] 6.2 steering beam	$0.88^{+.04}_{-.03}$	$1.26^{+.07}_{-.07}$	5.41	2.0

[a] Copper target located $2^{o}31'$ upstream from WTT.

[b] ± values -- etc. as on Table I, footnote 2.

[c] An attempt was made to move the beam orbit to a smaller radius for these runs; the smaller orbit was achieved, as determined on the control-room oscilloscope.

The proton-beam monitor is particularly susceptible to error (for our purposes) for conditions such as existed during Sets IV and V. Because this device records beam amplitude at only one instant during the acceleration cycle, typically just before maximum energy is attained, loss of beam prior to the sampling time goes unnoticed. Thus a large fraction of the beam might be lost between 4.1 and 5.7 Bev, while the proton monitor, set to measure at 5.7 Bev, records only the residual beam. This lost fraction would produce a significant stray-radiation field, and so counter measurements would not correlate well with proton monitor data. Such conditions are very likely to occur when beam steering is changed, especially if the changes are for so short a time that beam stability is not achieved; just this sort of situation existed here.

Immediately following these initial tests, the BF_3 central-monitor data became a regular part of Bevatron survey data. However, its response as well as the response of the other monitoring systems, has always been viewed with skepticism. When possible, several monitors are compared and in the frequent cases where there is disagreement among the monitors, an intelligent choice must be made as to which one should be used to interpret survey data.

The choice may be obvious: the proton beam monitor exhibits rf pickup or wide drift in calibration, and is disqualified. Another illustration of this case: a fast neutron counter is set up to be a monitor in an area for fast-neutron surveys in that area and relative levels are measured in this manner, as for the WTT maze survey (see page 39). There are times when the choice is made relative to previous data; there are also times when the choice must be made according to such qualitative evaluations as "how the machine is running".

For the exposures of three sets of Eastman Kodak NTA films during November - December 1955, the central monitor alone provided information related to the total accelerated protons. Ten calibrations checks were made during this period (see Table III), comparing the BF_3 counter response to beam amplitude as reported by accelerator operators viewing the control-room oscilloscope. All calibrations fall within ± 20%, and if one extreme value is discounted, the remaining 9 fall within ±10%. The utility of the central radiation monitor was greatly strengthened by this performance.

It is desirable that the central-monitor counter system be as stable and trouble-free as possible. Of particular importance is the high-voltage stability of the counter itself. Although the BF_3-filled proportional counter exhibits a useable plateau of up to 300-volts length as normally operated in our work, and is considered a thoroughly reliable counter, frequent calibration checks are necessary when reproducible results are to be expected. Such calibrations may be awkward to perform if, for example, the counter were in position at the top center of the Bevatron building.

A counter meeting these requirements is, with one reservation an ion chamber that has a thin deposit of U^{235} on alternate parallel plates. The chamber operates as a pulse counter, with its collection system arranged to

Table III

Comparison of central radiation monitor and control-room oscilloscope beam calibrations

Run No.	Date	Monitor Calibration (protons/1000 counts)
1	11/16	8.6×10^{10}
2	11/16	9.8×10^{10}
3	11/18	10.0×10^{10}
4	11/19	9.6×10^{10}
5	11/21	11.3×10^{10}
6	11/28	10.1×10^{10}
7	12/1	9.3×10^{10}
8	12/2	9.3×10^{10}
9	12/2	9.5×10^{10}
10	12/14	8.8×10^{10}
Average of 10 runs		9.6×10^{10}; all within ± 20%
Average of Runs 1 through 4 and 6 through 10		9.4×10^{10}; all within ± 10%

respond only to the electron component of ionization in the counting gas. Neutrons, primarily thermal and epithermal, are detected as fissions of U^{235}, and produce pulse heights several times those of competing events.

Such a chamber was available for use in this investigation. The chamber contains an array of 13 parallel circular plates 12 cm in diameter and spaced 1 cm apart. Seven plates are coated with U^{235} on both sides, and aluminum plates (6 in all) alternate with U^{235} plates in the array. High voltage is applied to the coated plates and the fission events are observed from ionization collected at the aluminum plates. A counting gas of Argon – 5% CO_2 at 1 atmosphere is used to give a favorable ratio of fission to alpha pulse height.

There are several advantages offered by this counter:

(a) The high-voltage plateau extends from 500 v upwards to at least 1000 volts (the upper limit of investigation).

(b) The argon – 5% CO_2 counting gas is more reliable in counters and much more easily handled outside counters than is BF_3 gas.

(c) The alpha-particle activity of U^{235} provides a built-in calibration facility which, incidentally, does not interfere with normal operation.

The single disadvantage is that fission pulses from the chamber are at a signal level of only 1 millivolt maximum. Because the problem of electrical pickup has always been serious at the Bevatron, doubt existed that these small pulses could be distinguished above the noise level. That this problem never proved to be serious is a tribute to the competence of William Goldsworthy of the Electronics Group, who designed and engineered the linear amplifier model V and companion low-noise preamplifier used for the U^{235} chamber. Both units were designed to minimize internal noise generation and noise pickup from external electrical sources. Typical operating conditions are:

Voltage gain:	40, 000
Fission pulse	40 v
Alpha pulse	10 v
Noise pulse	2 to 3 v

Initial work with the U^{235} chamber at the Bevatron was performed in July 1956 during another experiment that provided long periods of steady high-intensity beam with nearly constant operating conditions. Behavior of this chamber was investigated with respect to BF_3-13 and the proton-beam monitor. Both counters were located at the center of the magnet pit in an elevator that could be raised to any desired height in the building.

The curve plotted in Fig. 6 is an integral-bias curve for the U^{235} chamber taken at the 55-ft level; the points have been normalized with respect to BF_3-13 response. Alpha particle events can be seen to count at the 10-v level, and were observed up to 13 v. The lower point at 10 v represents the calculated neutron component at this level, based on the upper data point and a background run taken with no Bevatron beam. The point falls nicely on the curve as extrapolated back to the zero bias intercept.

The smooth curve indicated that the chamber system was working satisfactorily, and that a suitable operating point could be chosen somewhere on the relatively flat portion of the curve. At this time the rather high value of 35 v was selected, partly because electrical pickup problems would be minimized when the highest reasonable bias setting was used, and partly for the ease of comparison of the two counters when their counting ratio was near unity. That the curve does not show a more definite tendency toward the horizontal is to be expected, because the U^{235} coating is thick with respect to fission-fragment range.

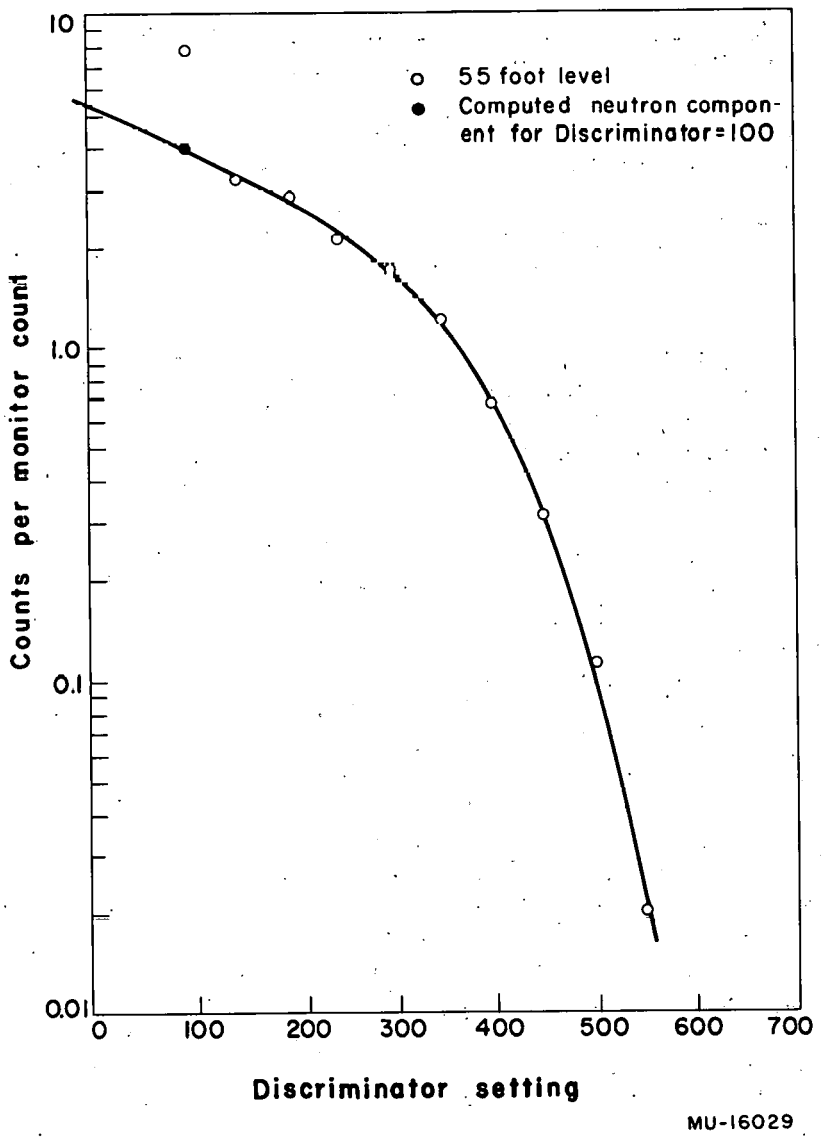

Fig. 6. U^{235} ion-chamber integral bias curve. High voltage is -600 volts.

Considerable additional data was obtained at this time relative to the reliability of this counting system; analysis of this information indicated that the desired stability could be expected from the system in its existing form.

Of particular interest are two other curves, Fig. 7 and Fig. 8, plotted from data taken during the July runs. Figure 7 shows the response of the U^{235} chamber relative to BF_3 counter response as a function of height in the building. The ratio U^{235}/BF_3 is seen to vary significantly with elevation; this is taken to mean that the neutron-energy spectrum changes with elevation. Fission in U^{235} occurs with fast neutrons more readily than does the (n, α) reaction in B^{10} with the same energy neutrons; thus if the two counters were placed in a mixed flux (both slow and fast neutrons) a U^{235} counter should show a relatively higher counting rate. The median plane of the Bevatron beam is at 15 ft, and the enhanced U^{235} response between 20 and 40 ft is thought to be associated with the high fast-neutron flux in this region. Depression of U^{235} response at lower levels is interpreted as a relative increase in thermal flux contributed by the concrete floor in the pit. Depression of U^{235} response at the highest levels is reasonably explained as the resultant of two factors: (a) decreased fast flux because of increased distance from source of fast neutrons (the median plane); (b) increased near-thermal flux because of the greatly increased area of the external concrete shield visibile at these heights, particularly the increase in area not obscured by the Bevatron magnet iron.

The curves shown in Fig. 8 depict response of both counters as a function of height relative to the proton-beam monitor. Two points of especial importance are noted:

(a) the counting rates above 60 ft are much higher than at any other level

(b) the counting rates show a great change between 50 and 60 ft.

The greater counting rates from (a) are associated with the increase in visible shield area, as explained above. The abrupt change in counting rates from (b) may be associated with the fact that at 55 ft. the counters emerge from a partial enclosure of steel I-beams, to travel in open air at all greater heights.

It must be emphasized that these explanations are based on rather meager evidence, but do seem reasonable in light of this evidence. There may be other explanations of the observed effects, and only through further experimental work will it be possible to determine which explanations describe the real situation.

Counting characteristics of the U^{235} chamber were more extensively investigated in October 1956, when a 10-channel differential pulse-height analyzer became available for this work.

The chamber was exposed to the neutron flux from a Po–Be neutron source; a 4-inch slab of paraffin was placed between source and counter to

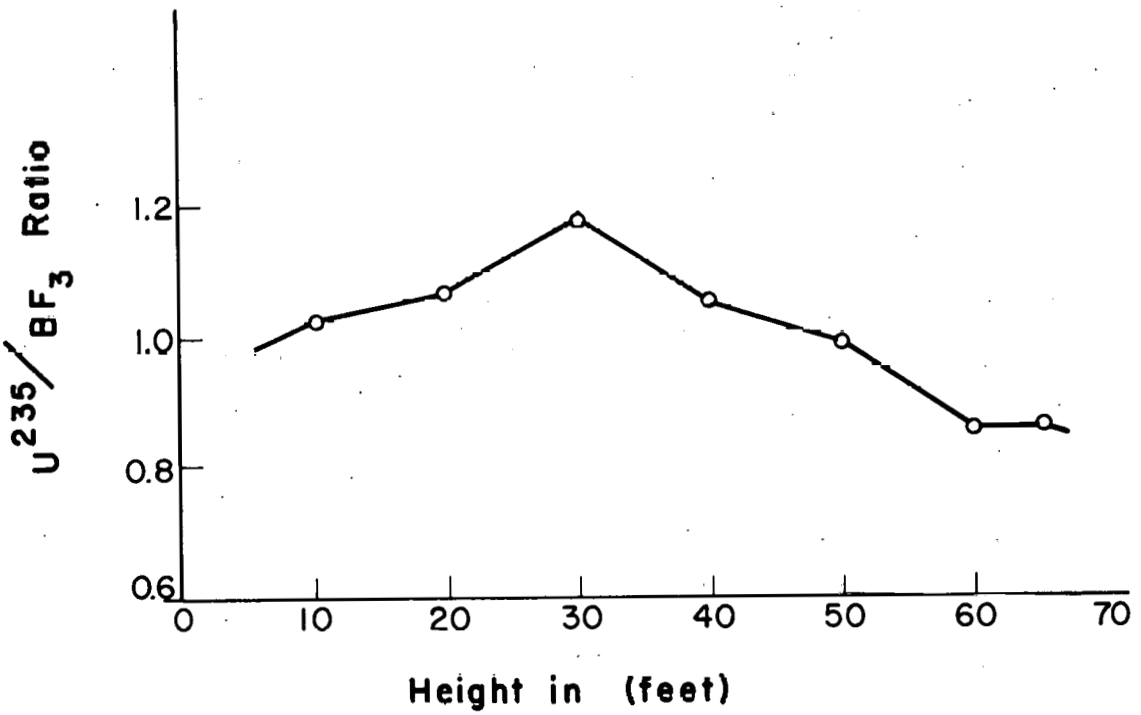

Fig. 7. Response of U^{235} ion chamber relative to BF_3 counter for various elevations along the central column.

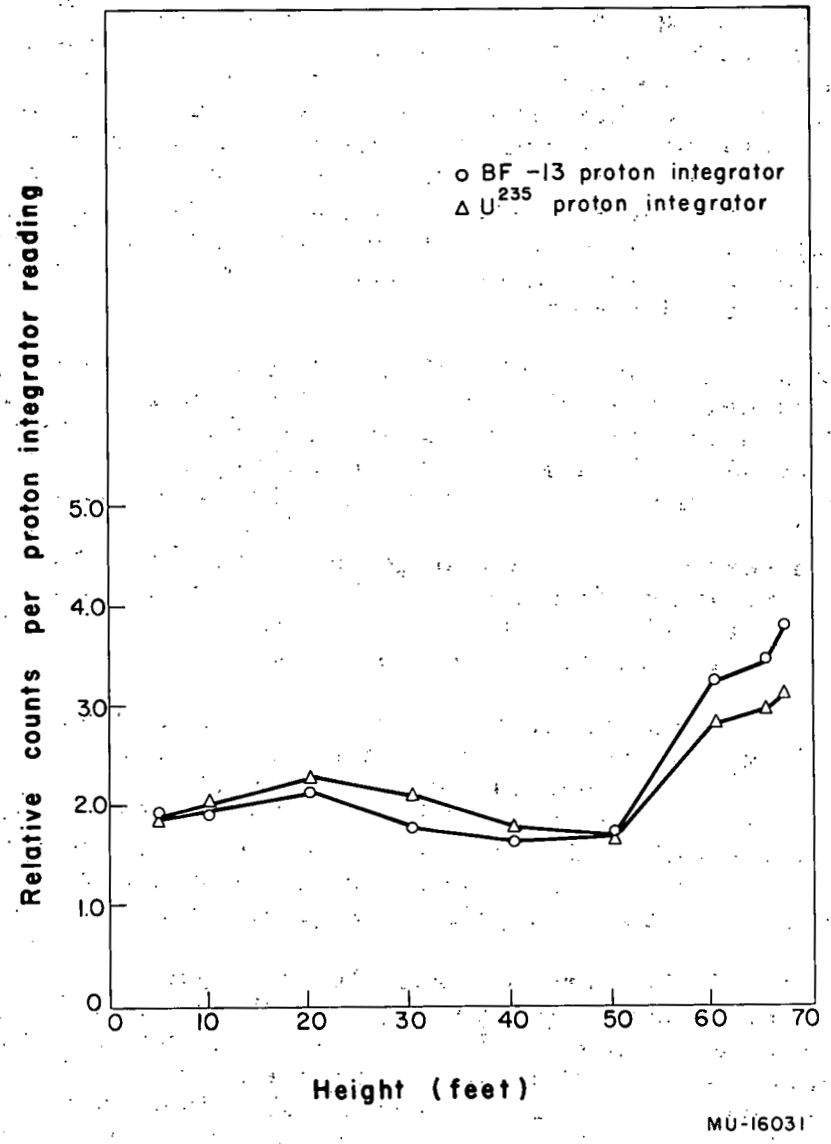

Fig. 8. Response of U^{235} ion chamber and BF_3 counter relative to the proton-beam integrator for various elevations along the central column.

provide a substantial thermal-neutron flux. The amplifier operated at approximately half-normal gain so that the end point of fission events could be conveniently observed. Data was taken in differential pulse-height form, to be converted to integral form as required. Chamber response was studied for a range of high voltage from 300 to 1000 volts in 50-volt increments. Figures 9 and 10 are respectively integral and differential bias curves for several high voltages. It is seen from Fig. 9 that for any given bias level below 10 volts, there is little change in counting rates over the interval 450 to 1000 volts. Because the chamber normally operates at 600 volts, the 600-volt curve is used as a base for the following performance analysis. In addition, a bias setting of 9 volts is chosen as an operating point: this setting corresponds to the higher setting of 13 volts used in practice with greater amplifier gain. Changes in the counting rate produced by changes in gain or voltage are:

High voltage decrease to 450 volts: -4% change in counting rate
High voltage decrease to 500 volts: -1% change in counting rate
High voltage increase to 1000 volts: +2% change in counting rate
Gain change of ± 10%: ± 4% change in counting rate
Discriminator change of ± 1 volt: ± 4% change in counting rate.

Stability of response to high-voltage change is thus satisfactory with the 600-volt battery box presently in use; this stability could be improved by an increase in battery voltage to 900 volts, but the gain in performance has not seemed justified in view of the increased size and weight of such a supply.

Stability against changes in gain and discriminator level, while adequate, leaves something to be desired. Both gain and discriminator level can be checked easily, and are checked at frequent intervals so that no significant change in sensitivity is permitted. Higher amplifier gain could be used so that a given absolute shift in discriminator level would produce a smaller percentage change in counting rate; however, it is desirable to work at as low a gain as possible. Some other solution is needed.

The differential bias curves of Fig. 10 do not show a peak in pulse-height distribution; however, it is possible that the peak would appear if the system gain were increased. Figure 11 shows both differential and integral bias curves taken with the gain increased a factor of 4. No peak is evident in the differential spectrum, even though pulses as small as those from α events are counted. The α counts are registered up to the 30-volt level. This behavior is interpreted as additional evidence that the U^{235} coating is much too thick.

It is proposed to prepare a new set of U^{235} coated plates having a thin active layer of the order of 0.5 mg/cm^2 thickness. Great improvement in system performance can be expected as a result, especially with respect to stability under gain-change and discriminator-level-change conditions. The improvement here comes as a result of a more unique pulse height produced by fission in the thin active layer.

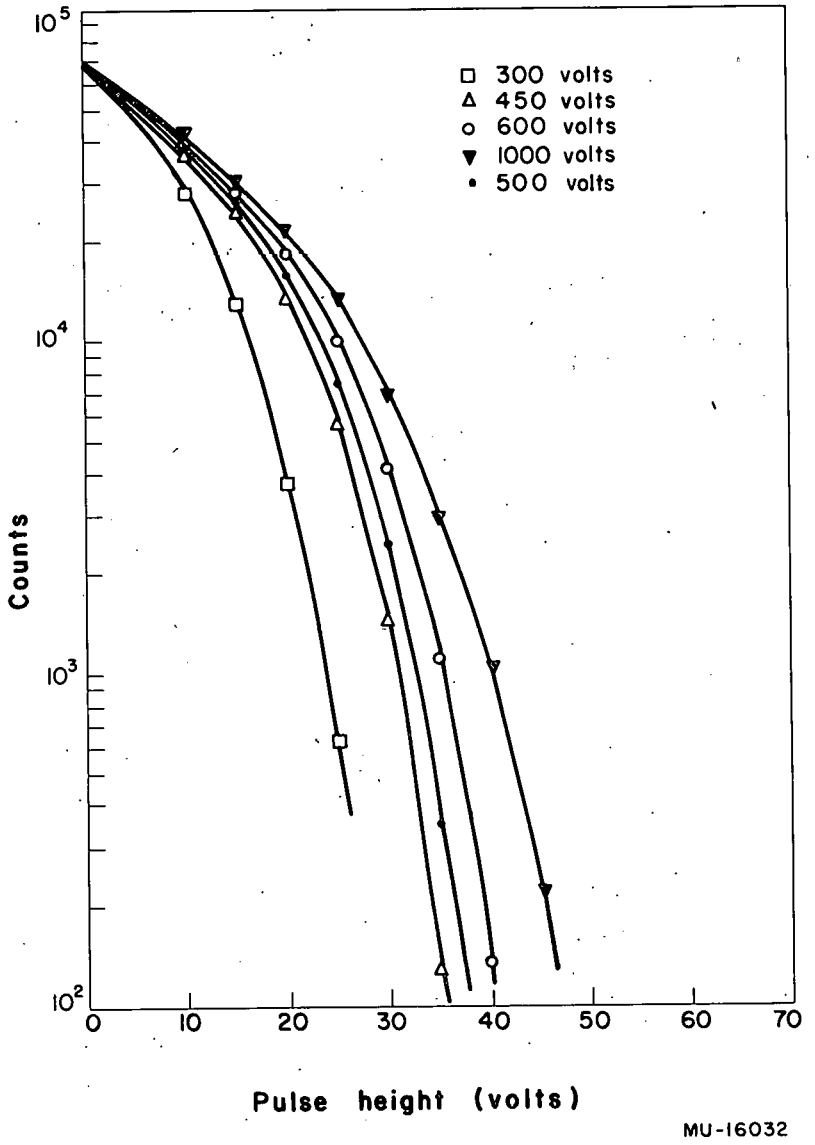

Fig. 9. U^{235} ion chamber integral-bias curves for several high voltages; neutrons are from moderated Po–Be source.

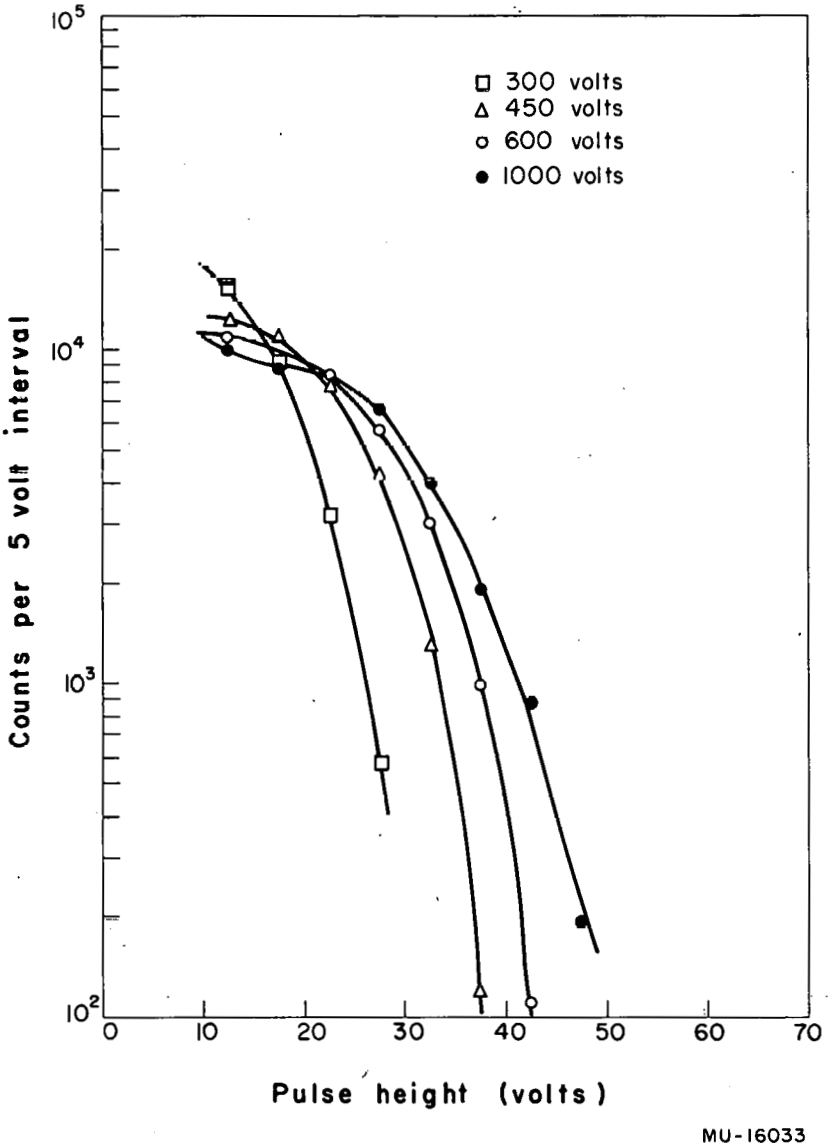

Fig. 10. U^{235} ion chamber differential bias curves for several high voltages; neutrons are from moderated Po–Be source.

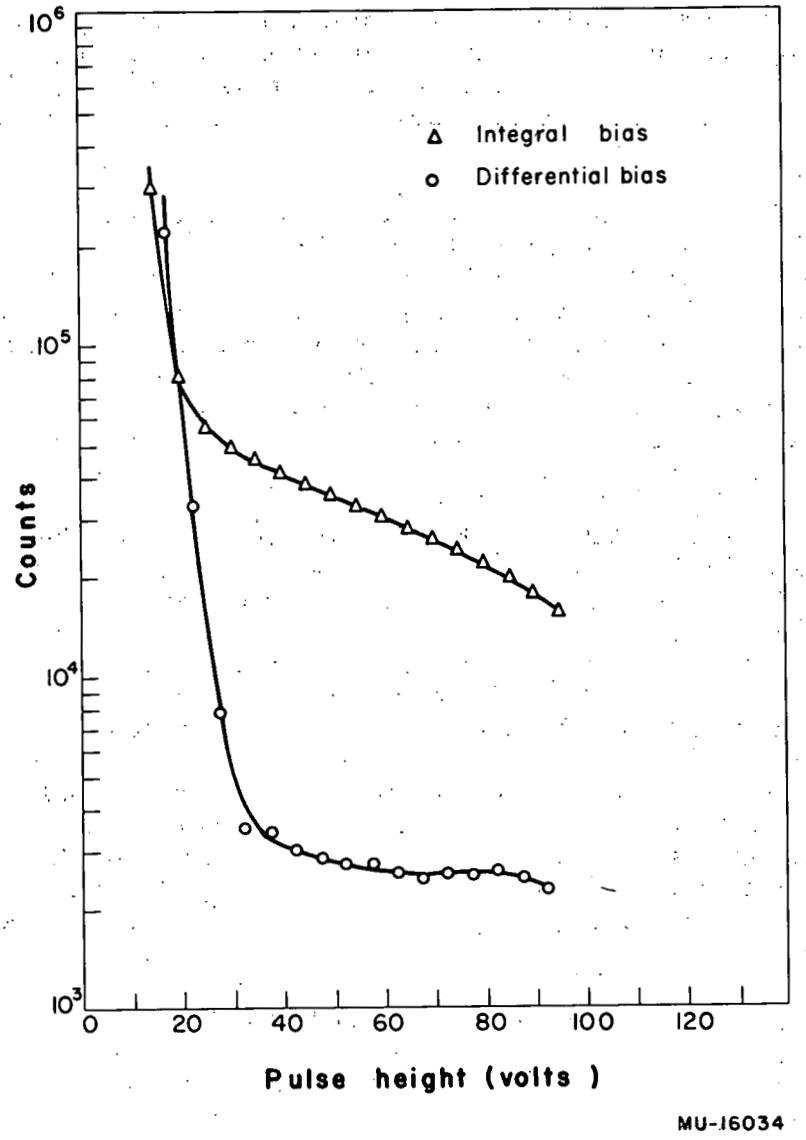

Fig. 11. U^{235} ion chamber differential- and integral-bias curves, showing position of α-pulse heights. High voltage is 600 volts.

Recent work at the Bevatron has shown the chamber to have a greater than needed sensitivity; in fact, the sensitivity has had to be reduced by wrapping cadmium around nearly 80% of the counter surface to prevent jamming of electronic counting equipment. A further improvement in performance can be effected by a reduction in number of plates in the chamber, thus decreasing chamber capacitance and thereby increasing output-signal level. The gain realized here may be as large as a factor of 5, which would permit considerable reduction in over-all amplification without a sacrifice of pulse height.

In summary, the centrally located slow-neutron detector has proved to be extremely valuable as a monitor for the stray radiation field of the Bevatron. Use of a U^{235}-fission ion chamber for this counter has been shown to be practical, and the counting system in its present form satisfies the criteria for accuracy and reliability now required, provided reasonable care is taken when the equipment is operated. Proposed improvements, to be made in the near future, should transform the system into a very stable and trouble-free counting system, one that requires a minimum of attention and maintainence. This is just the sort of equipment needed for the job.

Further experimentation with monitor counters is scheduled, and includes the use of other types of counters at the central location, as well as the use of counters at other locations. Indications are that no signal monitor counter can ever be devised to be the most useful one for all survey work; however, the central monitor has always provided useful information regarding the general over-all radiation-field level. Experience gained from use of monitors in different locations serves as a valuable body of information when plans are formulated to meet a new radiation-survey problem. Frequently, selection of the most useful monitor can be made from this previous data without the need for further experimentation. A great deal of time and effort is thus saved, and a relatively greater amount of time can be devoted to investigation of the problem at hand. Because we are always running short of survey time, such a time-saving procedure becomes an important item.

SURVEY MEASUREMENTS

General Approach

The radiation survey methods employed for the Bevatron can be viewed as an implementation of the general approach to Health Physics measurements in use at Berkeley. A basic premise to this approach is the consideration that the stray-radiation field exists as three general components: slow-neutron, fast-neutron, and gamma-ray fluxes. These components are to be measured individually, and the biological hazard associated with each is to be separately evaluated. The total biological hazard present at a given location can then be obtained additively from the three values.

Implicit in this method is the use of radiation detectors that can measure the three fluxes separately; ideally each detector would respond only to its appropriate component. In practice, the singularity of response

cannot be fully achieved; however, the system of detectors in general use exhibits a degree of uniqueness in response satisfactory for most survey work. For what may be termed regular survey work, the radiation field at a point is sufficiently known when three measurements are taken as follows:

(a) slow neutrons measured with a proportional counter which responds to slow-neutron flux density.

(b) fast neutrons measured with a proportional counter which responds to the product of energy × flux density.

(c) gamma rays and charged particles measured with a thin walled plastic ion chamber which responds to the ionization produced in the air within the chamber.

Special situations that arise from time to time may require more elaborate measuring techniques.

A wide variety of radiation detectors has seen service in Bevatron survey work; all are evaluated in terms of separable response to the three components. The three-detector system described above has been used extensively at the accelerator to determine radiation levels existing in all occupied areas. Other kinds of detectors have been used for such purposes as neutron energy-spectrum determination, simultaneous measurements at many widely separated points, or measurements in extremely high flux areas.

General radiation-level determinations have been made with two objectives in mind. The first can be stated as simply to determine that an area is safe for occupancy; this can be accomplished by noting that detector response is below that to be expected in the maximum permissible flux. The second and more difficult objective has been to correlate survey data with beam conditions in such a manner that the general radiation pattern can be constructed from these measurements, and that meaningful extrapolations of measured radiation levels can be made for proposed increases in beam magnitude. We have tried to keep to the principle that data taken at the present beam level should be good enough to provide useful predictions of the radiation levels expected with an increase in beam magnitude by a factor of 10. This is an important consideration because the Bevatron beam has steadily increased from an initial 10^7 protons per pulse (ppp) to the present 5×10^{10} ppp level, and will increase still further. Many occupied areas now receive a significant fraction of the maximum permissible fast-neutron flux. It is necessary to know the radiation levels as stated above, so that intelligent planning for these areas can be carried through with respect to shielding requirements and occupancy status when the anticipated higher beam magnitudes become a reality.

The analysis and interpretation of survey measurements contained in the following sections (pages 32-52) are based on data taken during the period March 1955 - February 1957. The measured levels of the three components of the radiation field are given in two different presentations.

The first scheme, (Fig. 14 for example) shows both the levels of fast-neutron flux and the actual survey-point locations on a plan view of the Bevatron building. The second scheme (Fig. 15 for example) shows much of the same data as Fig. 14, with the restriction that all data points are from survey locations at nearly the same radial distance from the machine. Both Bevatron and shielding are "unwrapped" in this presentation; the general trends of radiation levels are more clearly shown in this manner.

Fast-Neutron Surveys

The major effort in actual radiation surveying at the Bevatron has been, and continues to be, determination of the characteristics of the fast-neutron field. This state of affairs exists mainly because the fast-neutron component constitutes the greatest single health hazard, and also because of the difficulties encountered in detection of these neutrons under the conditions imposed by Bevatron operation. The nature of such problems has been discussed in previous sections.

A coherent picture of the fast-neutron field in the energy range 0.2 to 20 Mev has been obtained from polyethylene (PE)-lined proportional-counter data. There follows a summary and discussion of data so obtained, evaluated in light of the current understanding of the Bevatron as a source of stray radiation.

Figures 12 and 13 show the fast-neutron flux levels at two different elevations in the Bevatron building, measured at proton-beam energies between 5.7 and 6.1 Bev. The two elevations investigated are: beam level–8 ft above the floor–indicated by encircled numbers; and 5 ft above the shield top–20 ft above the floor–indicated by unmarked numbers. Surveyors and equipment were hoisted to the survey locations on a platform slung from an overhead traveling crane for these measurements. This survey was undertaken in the early days of Bevatron operation–as soon as the machine was capable of maintaining a reasonable steady beam at maximum energy and fairly high intensity. At the time the beam-monitor problem had not been satisfactorily solved, and in addition Bevatron operation was subject to considerable instability; thus the results of the survey must be taken as somewhat unreliable. The two points at which data was recorded on successive days illustrates this point; a disagreement of ~50% exists at these points - Bay 22/21 and Bay 6/5. However the general pattern as shown here is one that has been verified repeatedly by later measurements.

Radiation levels inside the magnet ring are very high, especially near the tangent tanks. Levels outside the ring behind the shield are naturally much lower, and are seen to increase significantly with elevation. Levels in the unshielded southeast quadrant (Bays 15, 16, and 17 were unshielded at this time) are noticeably higher than behind the main shield. Levels in the vicinity of the ETT are surprisingly high, approaching the magnitudes measured inside the magnet ring. It is reasoned that the combined effects of the injector and ETT produce the elevation in fast-neutron flux noted here.

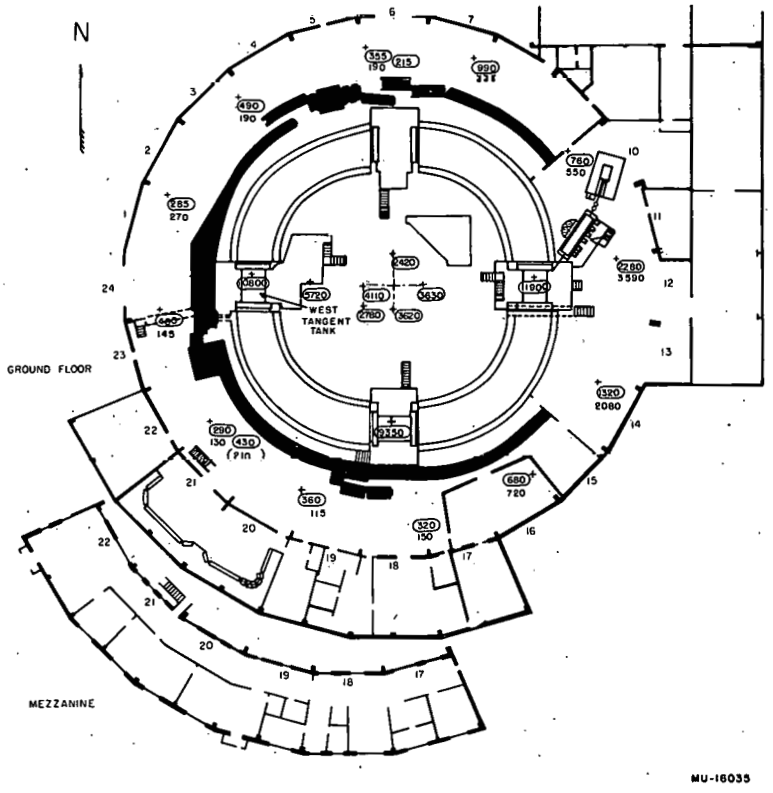

Fig. 12. Three-dimensional survey of fast-neutron energy flux levels for values of E_n between 0.2 and 20 Mev in Mev/cm^2/10^{10} protons measured at beam level (8 ft above floor) and 5 ft above shield top (encircled values). Values in parentheses are repeat measurements on successive days. Proton beam energy 5.7 to 6.2 Bev.

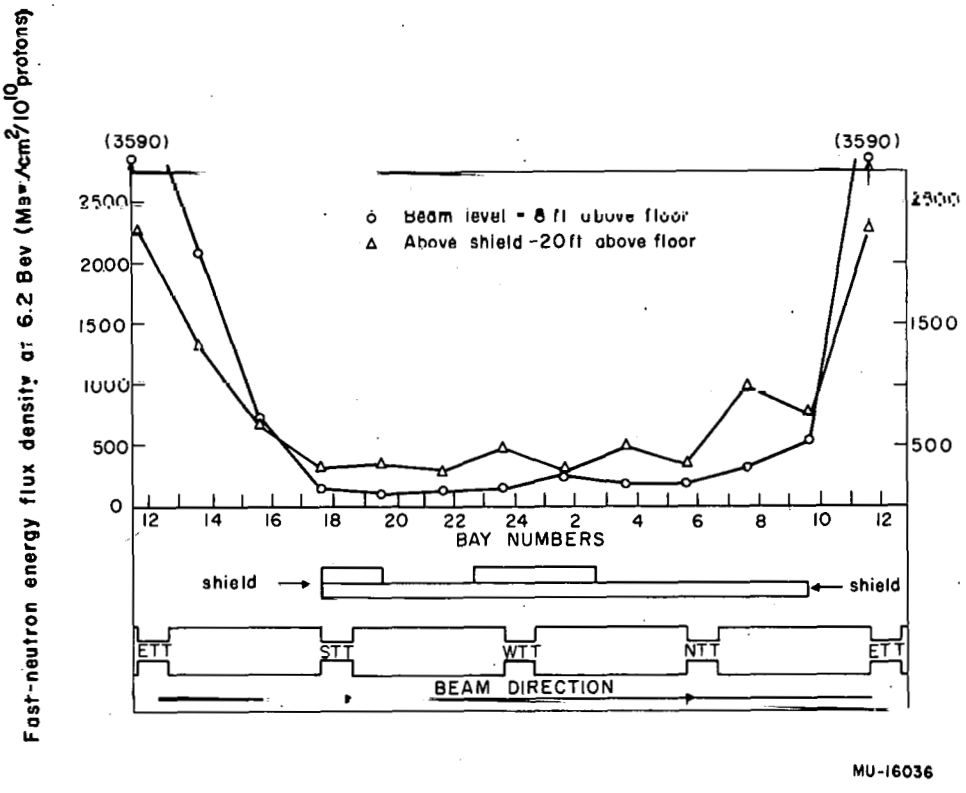

Fig. 13. Three-dimensional survey of fast-neutron energy flux levels for values of E_n between 0.2 and 20 Mev in Mev/cm^2/10^{10} protons measured at beam level (8 ft above floor) and 5 ft above shield top. Proton beam energy 5.7 to 6.2 Bev.

Figures 14, 15, and 16 show the measured distribution of fast-neutron flux for the magnet pit, ground floor, and mezzanine in terms of Mev/cm^2 per 10^{10} protons accelerated to 6.2 Bev. All these measurements were made during the interval August to November 1955, at a beam energy of 6.2 Bev with the main target located in or near the WTT. Maximum beam energy was chosen for survey measurements, because this energy would produce the highest radiation field per accelerated particle. Fortuitously, the longest periods of steady high-intensity beam time have also been at 6.2 Bev, a circumstance that has greatly aided survey work.

Levels in the magnet pit and in the unshielded southeast quadrant are quite high--much too high for continuous occupancy. Levels elsewhere on the ground floor behind the main shield are relatively uniform and low, and have permitted continuous occupancy of these areas. This statement must be qualified in the following manner, however. The safety of an area is dependent upon both the magnitude of accelerated beam and the pulse repetition rate. For the locally chosen fast-neutron tolerance rate of 20 Mev/cm^2 sec applied to the Bevatron, areas behind the shield are within this limit for beam magnitudes up to 2×10^{10} ppp at a repetition rate of 10 pulses per minute (the maximum rate for 6.2-Bev energy). Until shortly before the recent extended shutdown--February through June 1957--the Bevatron did not produce sustained periods of 6.2-Bev beam at greater than 2×10^{10} protons per pulse. However, immediately before shutdown, engineering improvements in the operational equipment made possible essentially continuous production of beam levels at 5 to 7×10^{10} ppp. In view of this development, and with the prospect of at least another two-fold increase of beam magnitude in the near future, the health-hazard problem becomes significant.

In a similar manner, the fast-neutron levels on the mezzanine (the present office space) are above the permissible limit for beam magnitudes greater than 2×10^{10} ppp. It is planned to abandon this area as space for continuous occupancy.

The effect of shielding configuration on radiation levels in the critical southwest quadrant, both on ground floor and mezzanine, is of primary importance. All measurements appearing in Fig. 14 were with one particular shield status. Since that time, both STT and WTT shielding have been augmented - the mazes have been deepened and partial roofs added to them; also, the southwest quadrant shield has been increased 4 ft in height. Preliminary results from an intensive study of the radiation field on the mezzanine show the effect of this additional shielding. (A complete report of the mezzanine surveys of October 1956 to February 1957 is in preparation.) At the Bay-20 location, Fig. 14 lists 43 Mev/cm^2 per 10^{10} protons, and the more recent data shows 48 Mev/cm^2 per 10^{10} protons with the top 4 ft removed from the southwest quadrant shield (conditions similar to those of the earlier survey). The level is decreased to 31 Mev/cm^2 per 10^{10} protons with this top 4 ft in place. A corresponding decrease in energy flux is likely on the main floor below. The gain, although significant, does not provide the margin of safety required to meet the operating conditions soon to be achieved, to say nothing of further beam increases now contemplated.

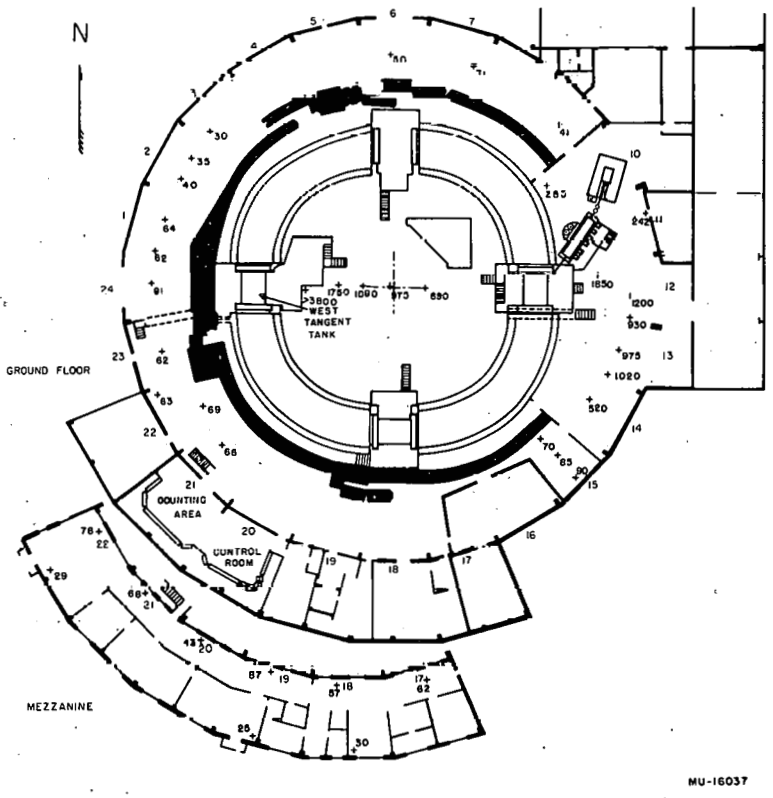

Fig. 14. Fast-neutron energy flux levels for values of E_n between 0.2 and 20 Mev in Mev/cm^2/10^{10} protons at 6.2 Bev. Main floor and mezzanine.

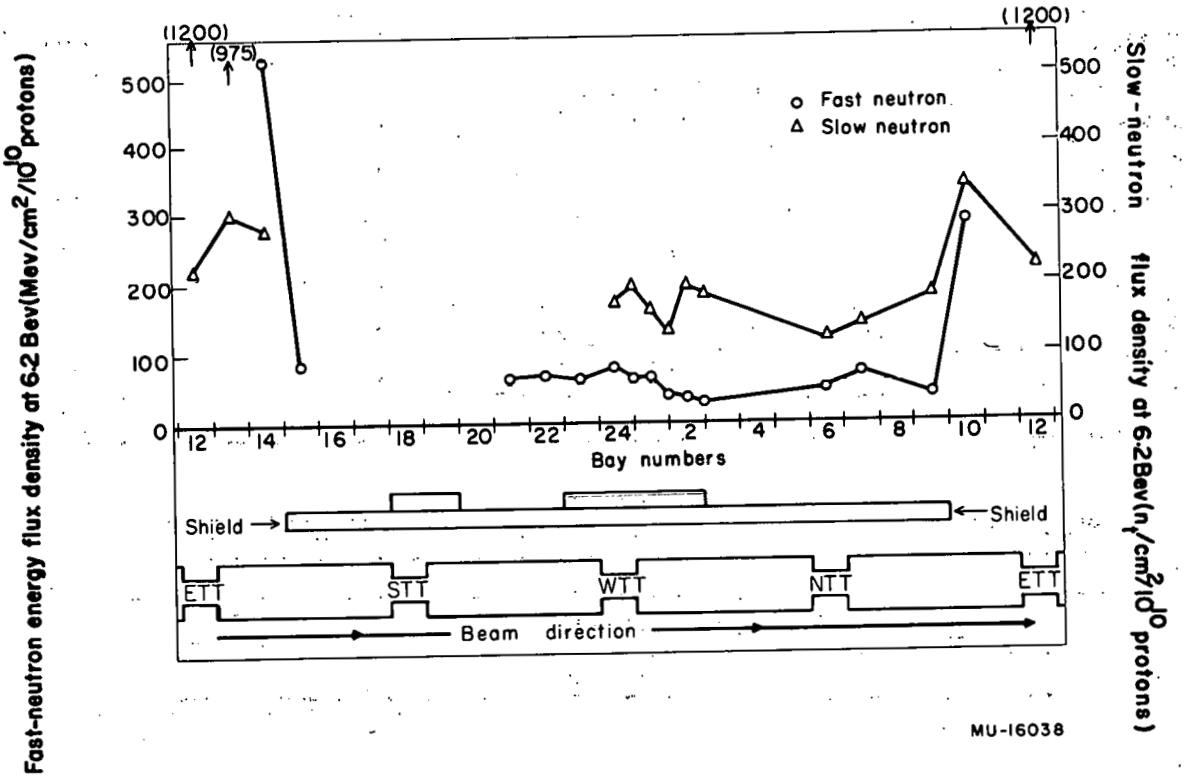

Fig. 15. Fast-neutron energy flux levels for values of E_n between 0.2 and 20 Mev in Mev/cm^2/10^{10} protons at 6.2 Bev. Main floor.

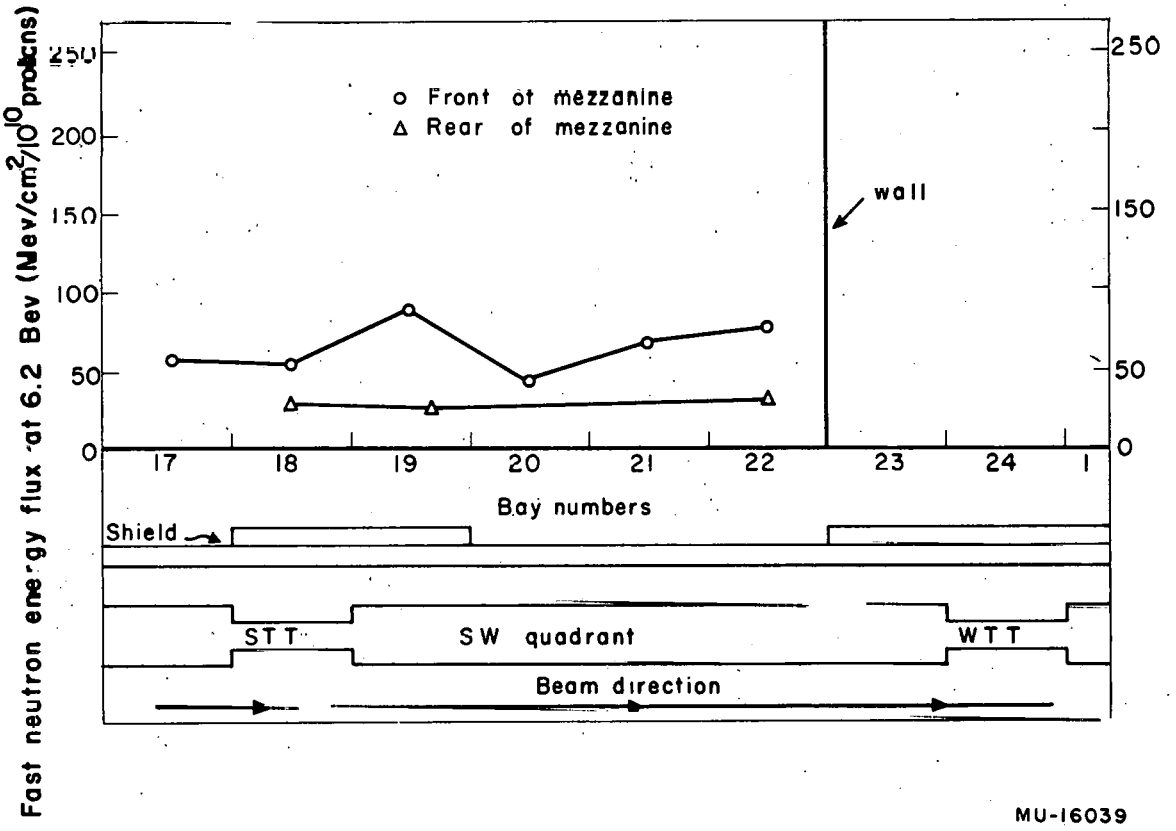

Fig. 16. Fast-neutron energy flux level for values of E_n between 0.2 and 20 Mev in Mev/cm^2/10^{10} protons at 6.2 Bev. Mezzanine.

There is convincing evidence that the major portion of fast flux seen outside and behind the shield is reflected down over the top of the shield. An increase in shield height would then seem to offer a solution. Unfortunately, at the southwest quadrant this process has already been carried nearly to the limit, both from the standpoint of floor loading and available height beneath the cranes. Some sort of roof shielding over the neutron-producing areas of the machine appears to be the most promising approach. Such shielding is difficult to support mechanically, and if required in certain areas, might prove very inconvenient from the experimental, operational, and maintainence aspects of the Bevatron.

Thus it is of great importance to identify these "hot spots", so that additional shielding can be utilized to maximum benefit in the least obtrusive manner. The technique of foil irradiation appears most promising as a survey procedure in this respect, as described in a later section of the report.

Considerable effort has been spent in rather specialized fast-neutron surveys. One example of this sort of survey work is the set of measurements taken in the vicinity of the access way to the WTT. At the time, late September 1955, the shield structure was such that the north end of the WTT could be seen from outside the shield. The problem was to determine whether a significant fast flux leaked out along this channel.

Figure 17 shows the WTT area with the relevant shield configuration, and the results of these measurements. It is evident that the fast-flux level is higher along the line of sight—approximately 50% higher than normal at Bay 22 Center, and increasingly higher as the WTT is approached. Further evidence of what may be called a neutron beam is provided by the two points inside the maze but outside this beam. One point is behind a shield block; the other, behind a considerable thickness of magnet iron. Both these points show much lower flux levels than do locations in the beam at corresponding distances from the WTT. The shielding in the WTT area has since been modified to eliminate this weakness as is apparent from an inspection of the shield layout depicted in Fig. 14.

The technique employed for these measurements is different from that normally used in survey work, but is especially adapted to detailed studies of local situations. The monitor counter is a polyethylene-lined proportional counter, which has been calibrated with respect to the proton beam. This counter remains at one position while the survey measurements are taken with a second polyethylene-lined counter. Data obtained with the second counter is then interpreted in terms of first counter response for each location surveyed. A more consistent pattern for fast-neutron flux distribution can be obtained in this manner than through the use of any other monitor system yet investigated.

The opportunity arose during this series of measurements to take data at two different beam energies with otherwise identical conditions of Bevatron operation. In Fig. 17 the flux levels for 4.8-Bev energy are encircled to distinguish them from the levels for 6.2-Bev energy. In all cases, the

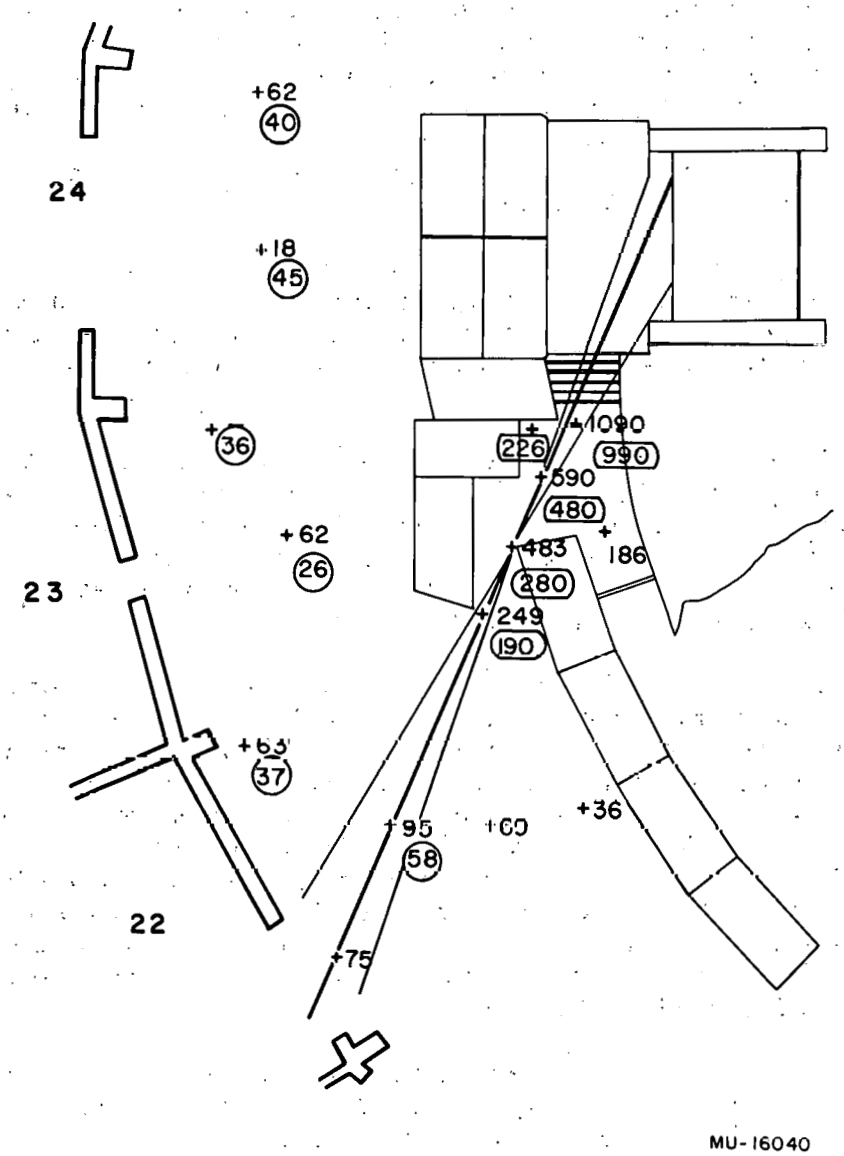

Fig. 17. Fast-neutron energy flux levels for values of E_n between 0.2 and 20 Mev in Mev/cm^2/10^{10} protons for 6.2-Bev protons and 4.8-Bev protons (encircled values) WTT area on Main floor.

neutron flux levels at reduced proton energy are lower than at full proton energy, as is to be expected. In most cases this decrease is greater than would be expected from a linear relationship between proton-beam energy and stray-neutron radiation.

Unfortunately there has been little opportunity to take data that pertains specifically to the relationship between beam energy and neutron production. Situations rarely arise wherein the experimenters change only the beam energy, while keeping other parameters constant; even these rare occasions are likely to be unsuitable for this purpose. Not enough is known of the effect of different targets or other operation changes to be able to correct for these and then state confidently that the remaining effect is due to a change in beam energy. The information at hand does tend to confirm the opinion that the measured stray-neutron production increases more rapidly than proton-beam energy; however, the differences seem to be relatively small. Thus there is no better assumption now available than the simple one that postulates linearity between beam energy and stray-neutron production.

No comprehensive studies of the fast-neutron field have been made for either lower beam energies or other target positions. Machine operation has not provided such opportunities. It should be noted that much of the early survey work was with reduced beam energy, but the data from such surveys (before March 1955) can not be used for these comparisons because of its unreliability. Both Bevatron instability and radiation-monitor difficulties contributed to this unreliability.

Those bits of data that bear on these matters and seem to be significant are included in Table IV. Group 1 indicates the magnitude of fast-neutron flux change for a large beam-energy change; this change should be fairly representative for the entire machine because of the counter location. It is interesting to note that slow-neutron flux measurements for these two conditions show a similar change, from 460 to 69 n_t/cm^2 per 10^{10} protons. Group 2 purports to show the change in the fast-neutron flux level at an unshielded location outside the magnet when different targets are active. It is not clear whether the targets are responsible for the large differences noticed, or whether the seemingly small adjustments in beam steering required to achieve the desired machine operation may have been largely responsible. Groups 3 and 4 show how a large hole in the shield opposite an active target influence local radiation levels. It is unlikely that such significant changes would have occurred if only the targets were changed. Group 5, taken with the same large beam hole and nearby target, illustrates the relative effectiveness of the shield against very-high-energy neutrons. It is expected that the 105 Mev/cm^2 registered at the lowest elevation would be typical for a beam-level observation if the shield were in place; thus the shield reduces the energy flux density by a factor of 200 under these conditions. The acutual reduction factor is probably even greater, since a substantial part of the fast neutron flux seen outside the shield is air scattered over the top.

Table IV

Fast-neutron survey data: miscellaneous measurements

Group	Survey location	Constant parameters	Variables	Range of variables	Energy flux density (Mev/cm^2/10^{10} protons)
1	Pit center	2.5° copper flip-up target	Proton energy	1.1 Bev	131
				6.2 Bev	975
2	Bay 14 center main Main floor	6.2 Bev	Target	2.5° copper flip-up target	520
				5° copper flip-up target	1050
				S1W emulsion	245
3	Bay 24 Main floor	6.2 Bev	Target and shielding	2.5° copper flip-up target, normal shield	81
				WIN 4-ft wide by 2-ft high beam hole in shield at Bay 24, center.	335
4	Bay 22 front and rear mezzanine	6.2 Bev	Target and shielding	2.5° copper flip-up target, normal shield	front 78 rear 29
				WIN 4-ft wide by 2-ft wide by 2-ft high beam hole in shield at Bay 24 center	front 190 rear 53
5	Bay 24 front at beam hole, 3 ft from shield	6.2 Bev, WIN target 4 × 2 ft beam hole	elevation	23 inches above floor	105
				43 inches above floor	136
				54 inches above floor	165
				64 inches above floor	238
				74 inches above floor, just below edge of hole	685
				96 inches above floor, at beam level	~20000

In summary, it may be said that the characteristics of the fast-neutron field revealed by these measuring techniques are both reasonable and understandable. There is strong evidence that shield thickness is adequate: no high radiation levels are detected at the median plane or outside the shield in the vicinity of targets. Rather, the intensity is observed to increase slowly with elevation from the floor to the shield top, indicating the presence of a strong air-scattered component outside the shield. Any median-plane peak is masked by this radiation. The tangent tanks are seen to be strong neutron-emitting areas; this effect is shown most clearly in the indium foil studies and is also evident from PE counter data. Many details need to be filled in to complete the fast-neutron field pattern; however, it is not expected that these details will alter the general characteristics as now understood.

Slow-Neutron Surveys

Slow-neutron survey data is taken with BF_3-filled proportional counters; the counters are unshielded and unmoderated in normal survey work. Partial or complete cadmium shields have been needed in some cases to reduce the count rate to a reasonable magnitude. All data reported here is in terms of the response of an unshielded counter. Although the coverage of slow-neutron surveys is not so complete as that for fast neutrons, it is considered adequate from the standpoint of health-physics requirements.

These measurements are usually taken at the same time as fast-neutron measurements. Such was the case for the slow-neutron flux levels shown in Figs. 18, 19, 20, 21, and 22 . The first of these, Figs. 18 and 19 show the results of the early Bevatron survey described on pages 32 - 33 . Figures 20, 21, and 22 show additional slow-neutron data, obtained at later times when both Bevatron operation and radiation monitoring facilities were more reliable. Slow neutron-levels are well below the 1500 n/cm^2-sec maximum permissible limit in all occupied areas; this is true even at the center of the magnet pit. The slow-neutron flux produces the least biological hazard of any of the three components into which Bevatron radiation is separated. It seems paradoxical that this is also the easiest flux to measure.

The slow-neutron field varies less rapidly from point to point than the fast-neutron field. This is to be expected, since the propagation of slow neutrons is primarily a diffusion process, and the magnet structure concrete shield combination constitutes an extended source of these neutrons. Additional information on the slow-neutron distribution pattern can be found in the Radiation Monitor section, (pages 21 - 23 and Fig. 8) showing an elevation study at the magnet-pit center, and in the Foil Techniques section (pages 62 - 70 and Fig. 28) showing a radial study at Bay 20.

Ionizing-Radiation Surveys

Plastic-walled air ionization chambers are used to measure the ionizing radiation. These measurements are taken simultaneously with the slow- and fast-neutron data whenever possible. Figures 23 and 24 show the results of the early Bevatron survey (see pages 32-33); Figure 25 shows measurements obtained in later surveys.

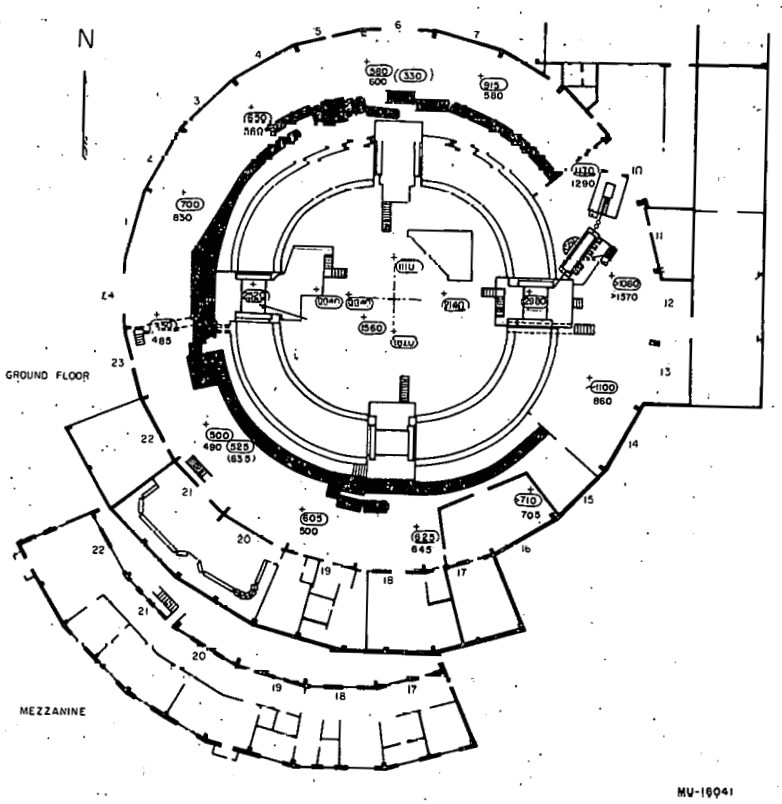

Fig. 18. Three-dimensional survey of slow-neutron flux levels in neutrons/cm^2/10^{10} protons measured at beam level- (8ft above floor) and 5 ft above shield top (encircled values). Values in parentheses are repeat measurements on successive days. Proton beam energy 5.7 to 6.2 Bev.

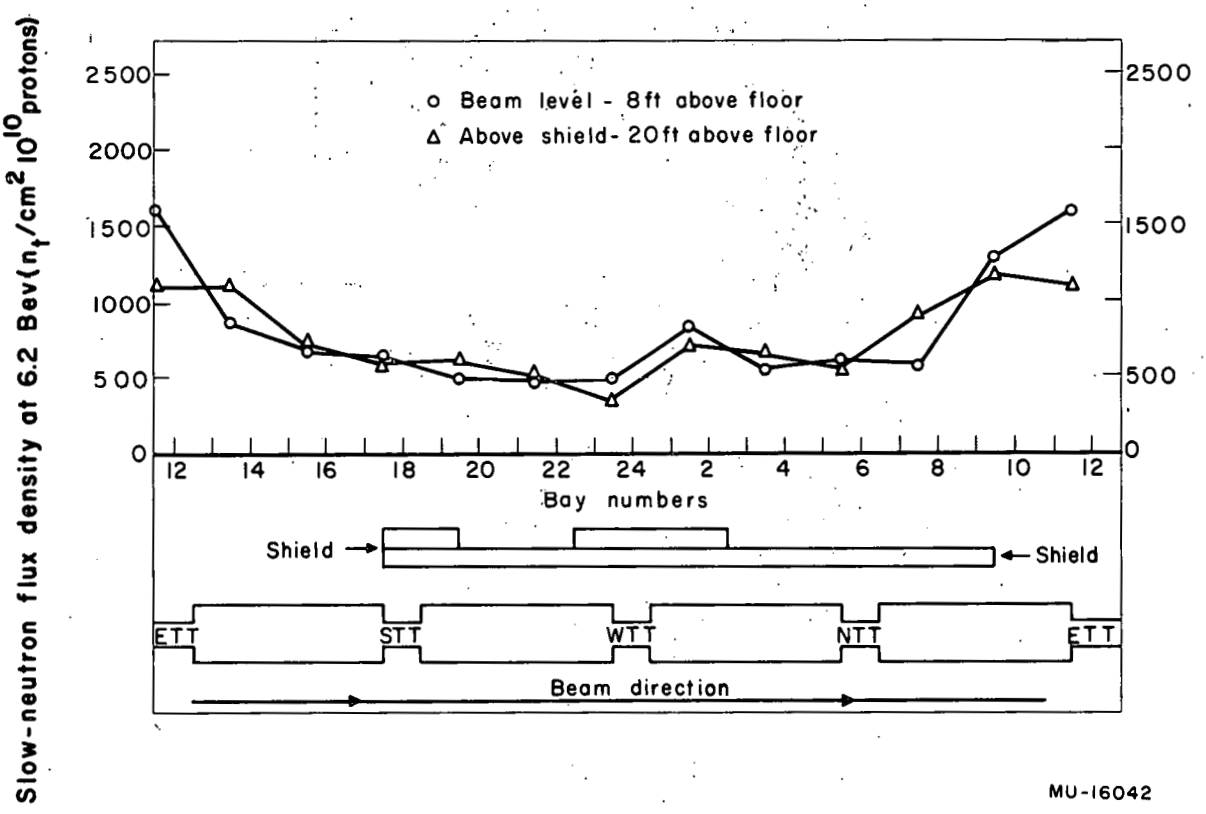

Fig. 19. Three-dimensional survey of slow-neutron flux levels in neutrons/cm^2/10^{10} protons measured at beam level - (8 ft above floor) and 5 ft above shield top. Proton beam energy 5.7 to 6.2 Bev.

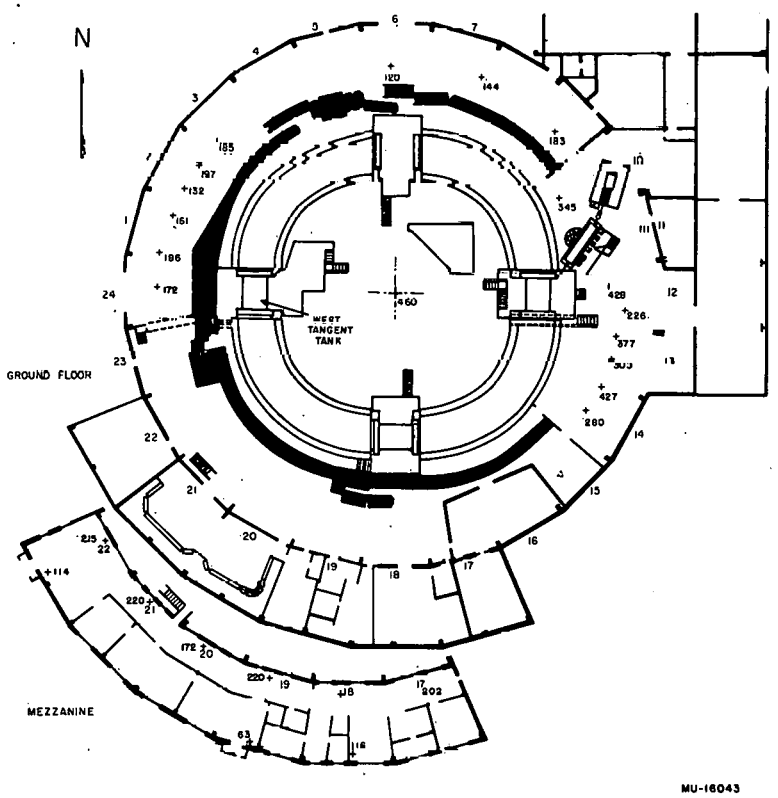

Fig. 20. Slow-neutron flux levels in neutrons/$cm^2/10^{10}$ protons at 6.2 Bev on Main floor and mezzanine.

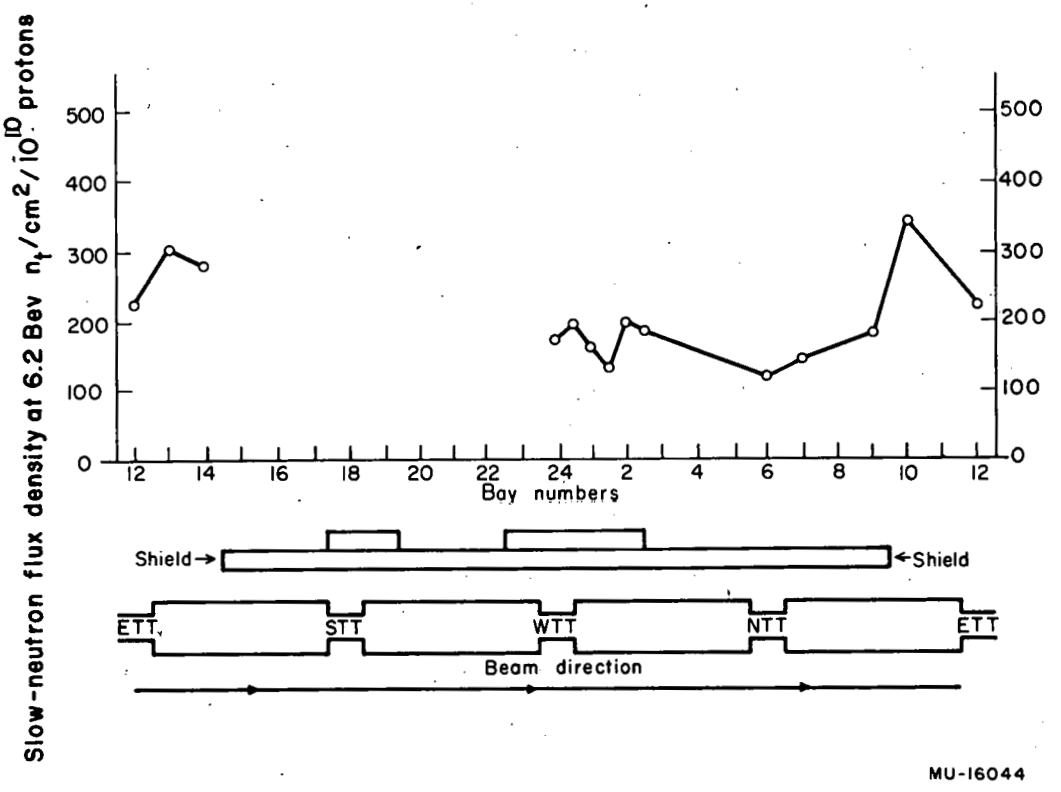

Fig. 21. Slow-neutron flux levels in neutrons/$cm^2/10^{10}$ protons at 6.2 Bev on Main floor.

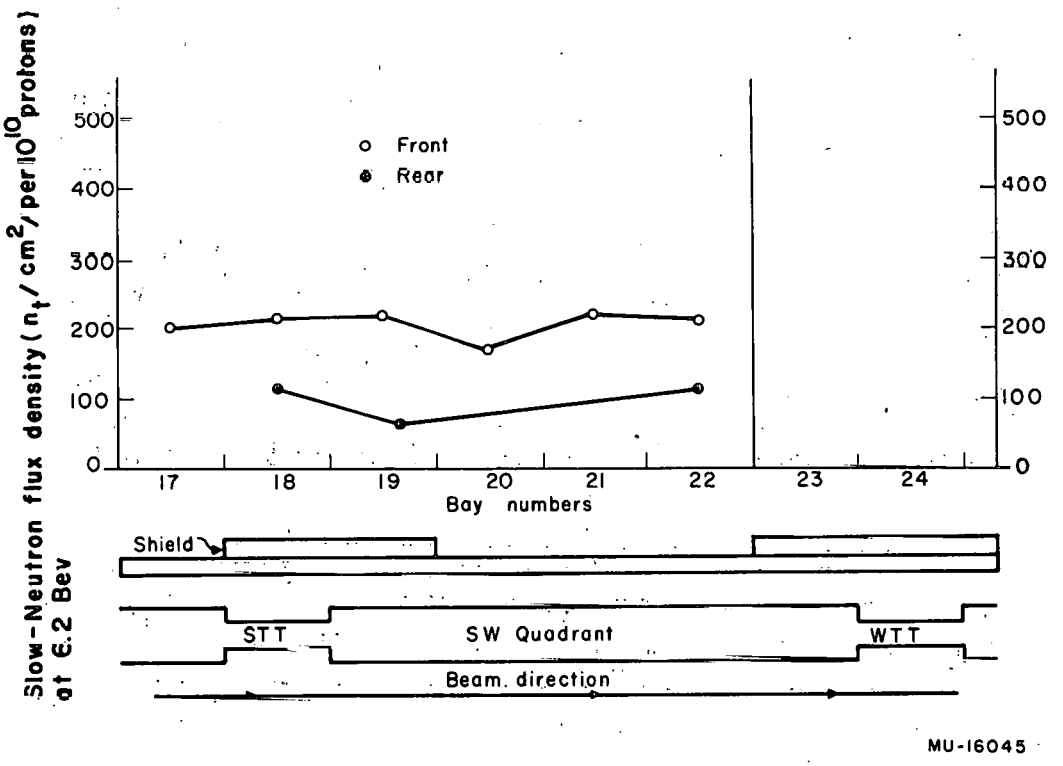

Fig. 22. Slow-neutron flux levels in neutrons/cm^2/10^{10} protons at 6.2 Bev on mezzanine.

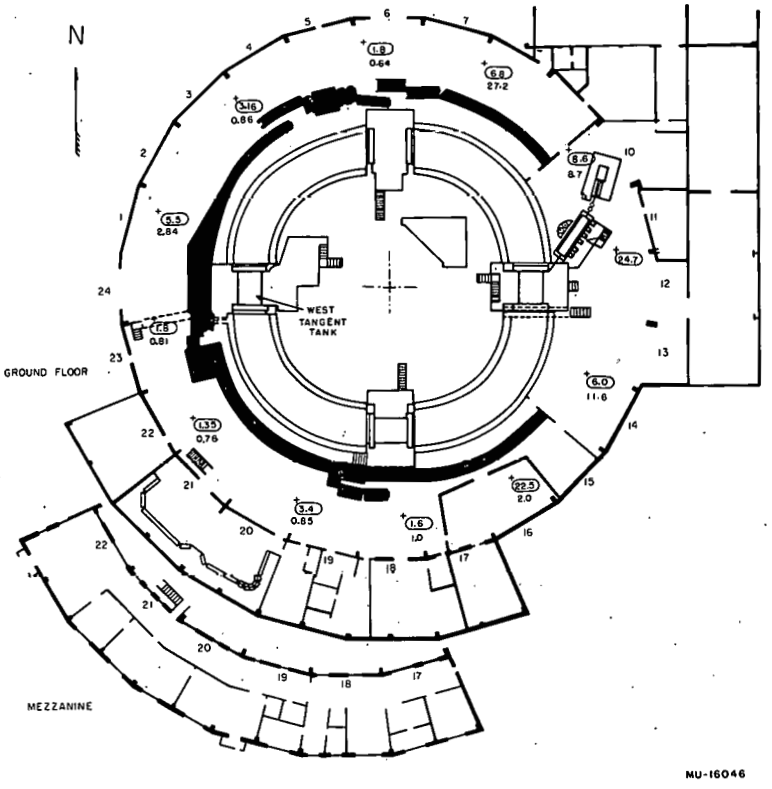

Fig. 23. Ionization-chamber measurements in microroentgens/10^{10} protons at 5.7 to 6.2 Bev. Three-dimensional study at beam level (8 ft level) and 5 ft above shield top (encircled values).

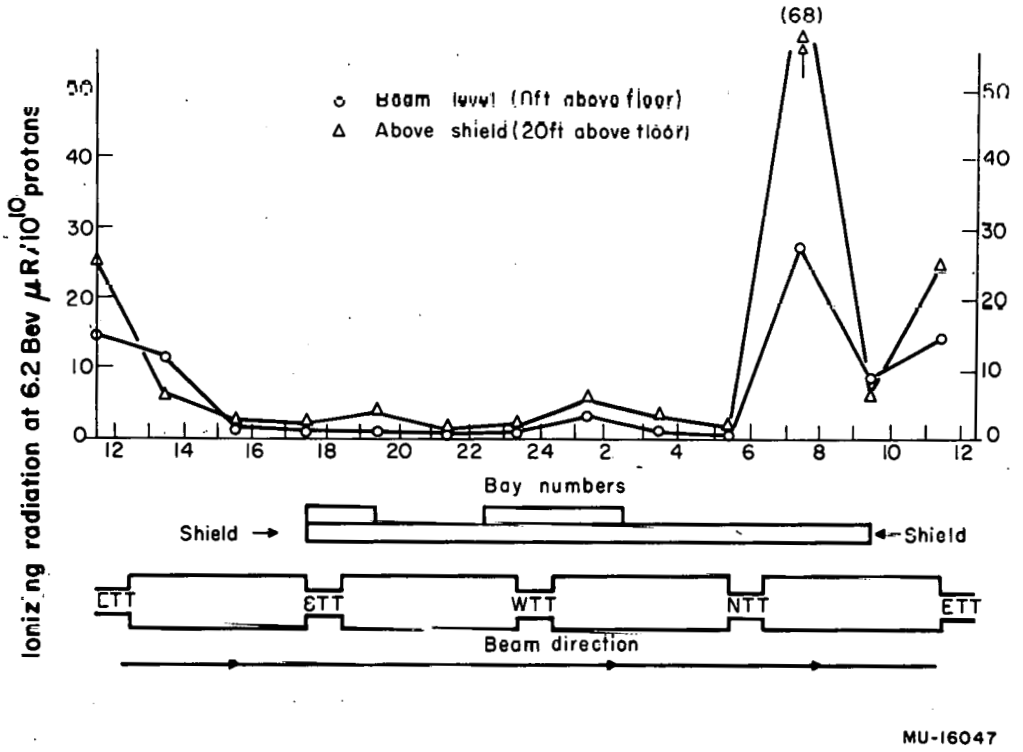

Fig. 24. Ionization-chamber measurements in microroentgens/10^{10} protons at 5.7 to 6.2 Bev. Three-dimensional study at beam level (8 ft level) and 5 ft above shield top.

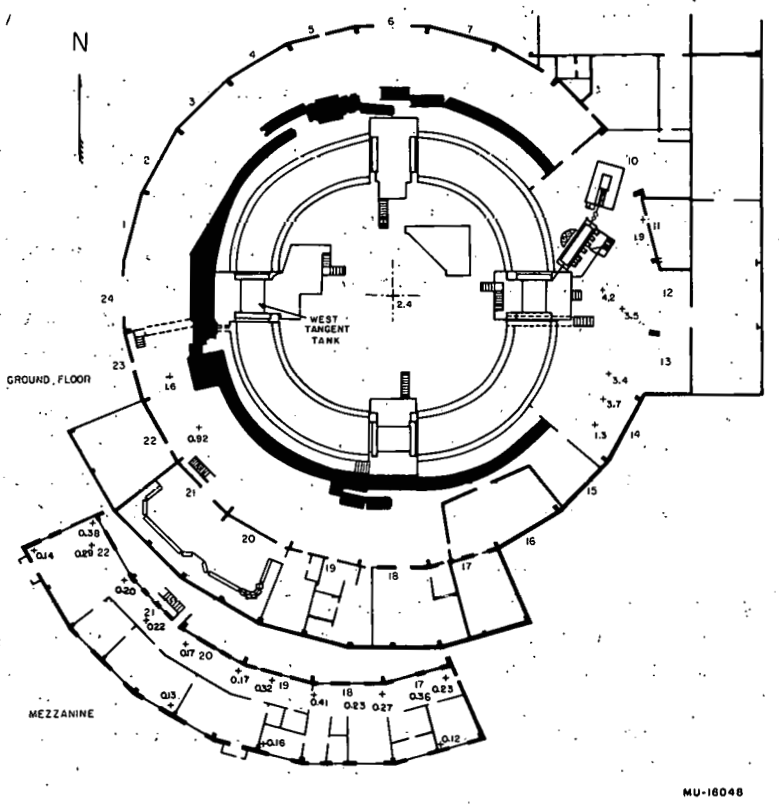

Fig. 25. Ionization-chamber measurements in microroentgens/10^{10} protons at 6.2 Bev on main floor and mezzaine.

These later measurements do not show a higher radiation intensity on the mezzanine compared to the main floor; to the contrary, a decrease is noted. This seems reasonable if a significant fraction of the total ionization detected is produced by gamma rays from thermal-neutron capture in the concrete of the shield and main floor; the mezzanine is a considerable distance from all this concrete.

NEUTRON-ENERGY DETERMINATION

Because the biological hazard associated with a given neutron flux is dependent upon the energy carried by the neutrons, the most realistic evaluation of this hazard can be made only when the neutron energy spectrum is known. It is true that the hazard from an unknown neutron flux can be evaluated without this specific information, if we take into account such factors as neutron-producing reactions, shielding configurations, relevant survey data, and previous experience with similar situations. A conservative interpretation of all these factors can then yield an estimate of the biological hazard; an evaluation so constructed will in general be an overestimate. This is obviously not the best way to proceed, particularly because the hazard can in some cases be greatly overestimated to needlessly restrict or even deny the use of accelerator facilities to operators and experimenters.

Once the neutron spectrum is determined, then the more reasonable estimate of biological hazard can be made. In addition, a clearer understanding of shielding problems can be achieved, and a better knowledge of the actual neutron-production mechanisms will be possible. For these reasons much effort has been, and will continue to be, directed toward neutron energy-spectrum determination. The techniques employed, along with significant results obtained are described in this section.

Paraffin Buildup

One technique that yields information related to the energy spectrum of a neutron flux employs various thicknesses of moderator surrounding a thermal-neutron detector. Paraffin cylinders of wall thickness ranging from 0.25 to 6 inches serve as moderators, while a standard BF_3 counter detects those neutrons thermalized in the surrounding jackets. A cadmium cover may be placed around the assembly to suppress sensitivity to the thermal-neutron component of the incident flux.

A plot of count rate versus moderator thickness generates a curve that has a shape dependent upon the energy spectrum of the incident neutron flux. As paraffin thickness increases, the curve rises to a broad maximum and then falls off steadily. When a mixed flux of fast and slow neutrons is examined, the rise of the curve is related to the abundance of epithermal and resonance neutrons, the position of the peak is associated with the energy interval containing the greatest number of fast neutrons, and the nature of fall-off beyond the peak is related to the neutron population with energies equal to or greater than the energy appropriate to the peak position.

Unfortunately the energy sensitivity of this method is quite poor, and quantitative results are difficult to deduce from the curves. The most useful information so far obtained has come by way of a comparison between Bevatron neutron curves and (α, n) neutron-source curves. Figure 26 shows the comparison of one Bevatron curve (Fig. 27) with curves from Po-Li, mock-fission, and Po-Be neutron sources. All curves are normalized to a peak count rate of 100. (The thin jackets were not available for source curve data.) All curves represent response of the apparatus when completely shielded by 0.030-inch cadmium. It should be mentioned that the zero thickness points for the three sources lie between 0.4 and 0.5, a decade below the Bevatron zero point. An interpretation of these curves attributes the following characteristics to the Bevatron neutron field at this mezzanine location:

(a) There exists a large epithermal and resonance flux.

(b) The mean energy of all neutrons above the cadmium cutoff is somewhat below 400 Kev (the mean energy of Po-Li neutrons), and probably between 200 and 400 kev.

(c) There exists a high energy tail as evidenced by the decreased rate of fall-off for the thickest jackets.

These conclusions are consistent with the Bevatron neutron-field characteristics as currently understood.

A second Bevatron curve is shown in Fig. 28; the location for this data is on the main floor, Bay 21, almost directly below the mezzanine station of Fig. 27. The curve shows a more rapid rise and a more rapid fall-off than the mezzanine curve. This behavior is in accord with a pattern for the neutron field that presumes the major source of fast neutrons outside the main shield to result from air scattering over the shield top. One would then expect a shift to the left for curves taken on the main floor, corresponding to a neutron flux relatively richer in the low-energy region and depleted at the high-energy end. Data for Fig. 27 and Fig. 28 appear in Table V.

Both Bevatron curves were obtained through use of a special monitor counter. A BF_3 counter in a paraffin jacket located near the apparatus proved to be the only means for correlating successive runs to produce a smooth buildup curve. The monitor counter was in a 2-inch-thick paraffin jacket and located 4 ft from the buildup counter for these runs.

If was possible to relate the Bay-21 data to the circulating proton beam; the peak of the curve of Fig. 28 represents a buildup counter response of 750 counts per 10^{10} protons accelerated to 6.2 Bev. The fast-neutron energy flux density measured with a PE-lined counter at this location is about 60 Mev/cm^2 per 10^{10} protons; the counter would produce 2 to 3 counts per 10^{10} protons at the discriminator settings normally used to take survey data.

The great increase in sensitivity of the moderated BF_3 counter relative to a PE-lined counter is obvious from these numbers. A second distinct

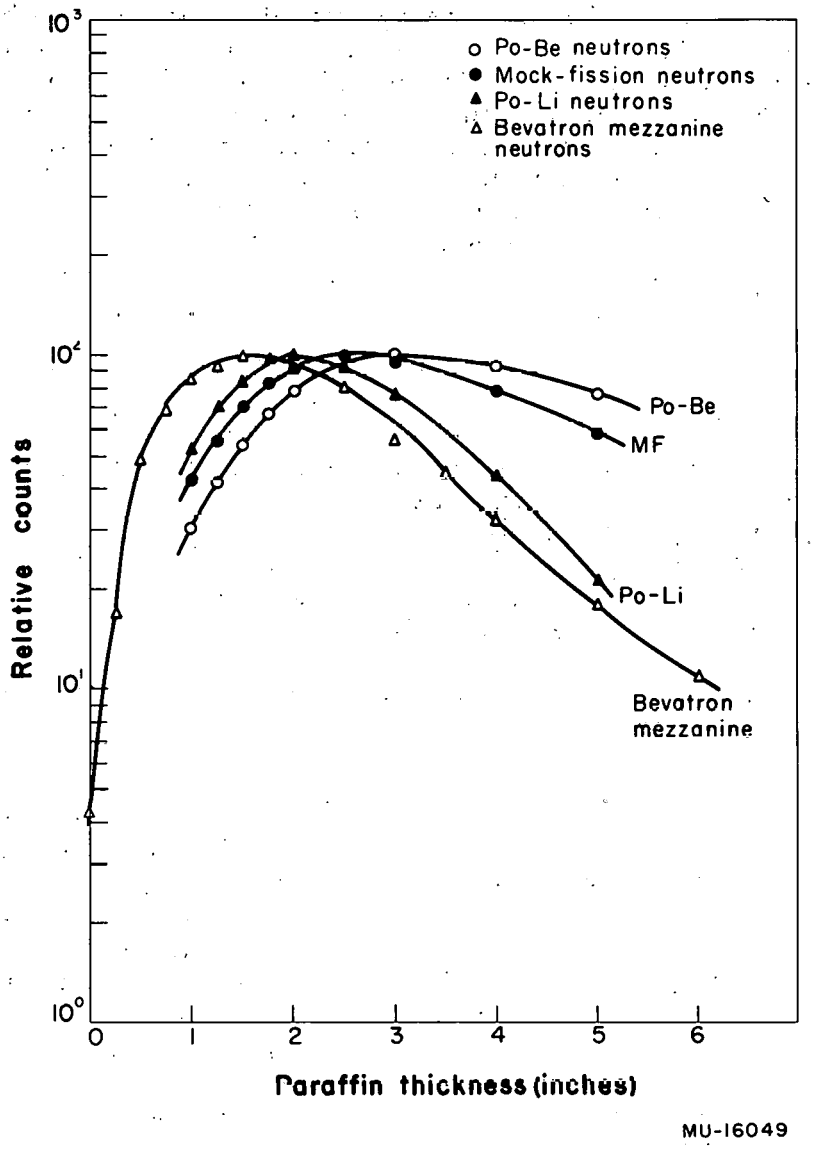

Fig. 26. Paraffin build-up curves; neutron-source curves and Bevatron mezzainine curve.

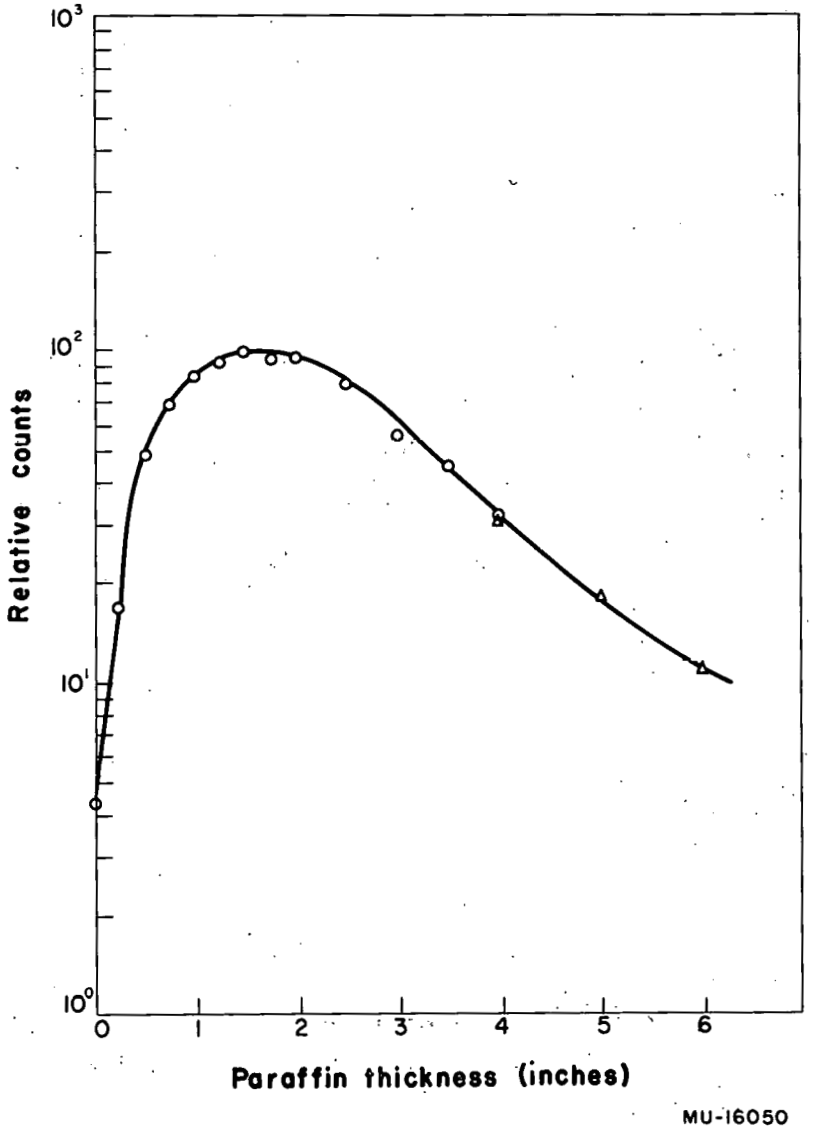

Fig. 27. Paraffin build-up curve for Bevatron mezzaine at 6.2 Bev and $\sim 5 \times 10^9$ protons/pulse with WIN target at I_{30}.

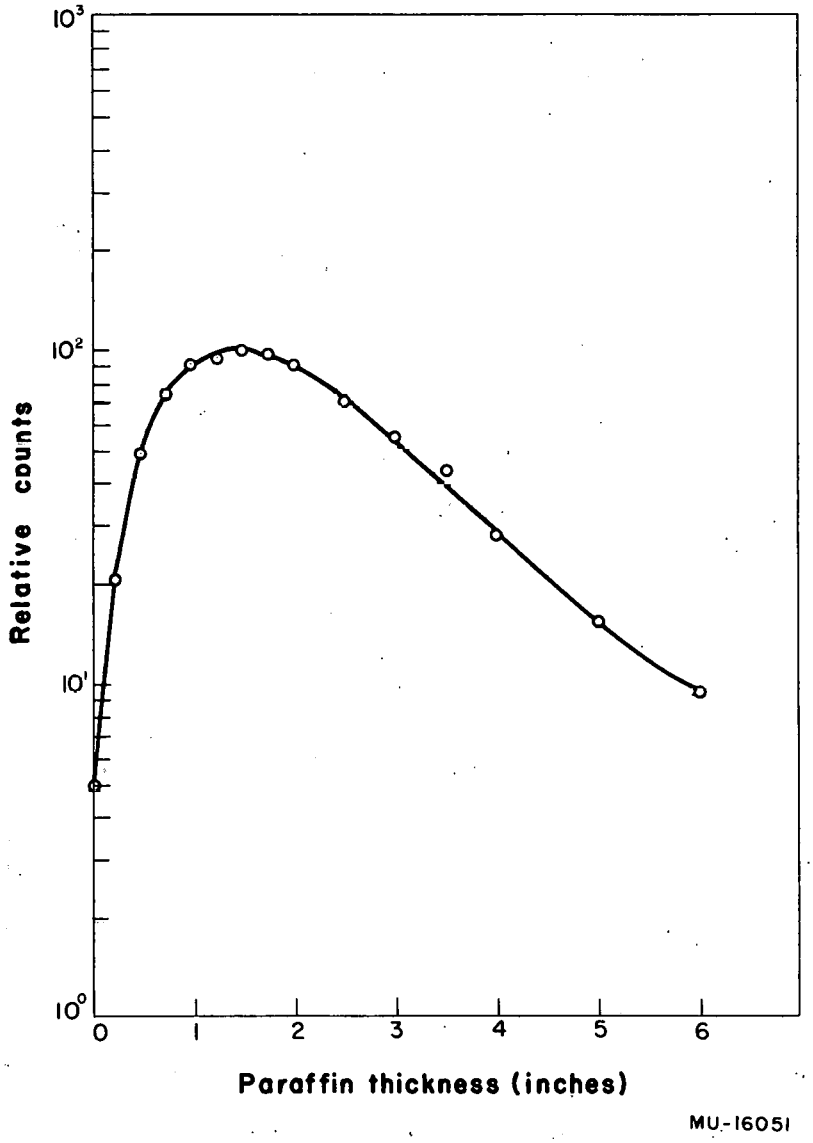

Fig. 28. Paraffin build-up curve for Bevatron main floor at 6.2 Bev and $\sim 5 \times 10^9$ protons/pulse with 2.5° copper target at I_{30}.

Table V

Paraffin build-up data for the two Bevatron curves.

Paraffin thickness (inches)	Mezzanine - B22FC		Main floor - B21RC[a]	
	Counts per mon. count	Normalized counts per mon.	Counts per mon. count	Normalized counts per mon.
0	0.66	4.3	0.76	4.97
1/4	2.59	16.9	3.11	20.4
1/2	7.48	48.8	7.42	48.5
3/4	10.7	69.6	11.3	73.8
1	13.0	84.8	13.7	89.6
1-1/4	14.2	92.8	14.7	96.2
1-1/2	15.3	100.0	15.3	100.0
1-3/4	14.8	96.1	14.9	97.5
2	14.7	95.9	14.1	92.2
2-1/2	12.3	79.9	10.6	69.6
3	8.52	55.7	8.32	54.5
3-1/2	6.85	44.7	6.65	43.5
4	4.93	32.2	4.27	27.9
5	2.65	17.7	2.31	15.2
6	1.64	10.9	1.44	9.4

[a]Calibration of monitor vs proton beam for main floor, data only; 500 mon. counts per 10^{10} protons at 6.2 Bev. Each point represents 5000 mon. counts.

advantage of the BF_3-counter method is its ability to discriminate sharply between neutron and gamma events. A careful study of the properties of moderated BF_3 counter configurations in known energy neutron fluxes is planned. It is hoped that through these studies methods will be developed to improve the energy resolution of the system, and that more quantitative interpretations for the rising and falling characteristics of the curves will be learned. The need for a method of fast-neutron flux measurement with the efficiency of this type system becomes more urgent as the demand increases for the accurate determination of lower and lower levels.

Two-Counter Method

The response characteristics of the Hansen-McKibben counter and the PE-lined counter can be utilized together to provide neutron-energy spectrum information. Because the Hansen-McKibben counter responds to flux density and the PE counter responds to energy flux density, a ratio of the two count rates yields a value $\overline{E}$ for neutron energy. This $\overline{E}$ value is the single neutron energy that would have produced the observed count rate in both counters from an $\overline{E}$ flux equal in intensity to the unknown flux.

The two counters are first exposed to Po-Be neutrons (mean energy taken to be 4.6-Mev per neutron) from a calibrated source to determine the constants of proportionality that convert count rates into neutron-flux quantities. Counter characteristics are then taken to be as follows:

(a) PE-lined counter– 15 Mev/cm^2 neutron flux density incident normal to counter produces one count, valid for a neutron energy range of 0.1 to 20 Mev.

(b) Hansen-McKibben counter– 0.42 n/cm^2 flux incident on face of counter produces one count, valid for a neutron energy range from thermal to 20 Mev.

The counters are exposed simultaneously at a location in the unknown flux, and the value for $\overline{E}$ is calculated.

A value for $\overline{E}$ determined by this method in survey situations is approximate for a variety of reasons. Among these are loss of sensitivity of Hansen-McKibben counter at both low and high neutron energies, the approximate nature of the PE-lined counter proportionality constant, and the directional response characteristics of both counters. Because the stray neutron flux outside a massive shield is relatively rich in low-energy neutrons, and the flux is not strongly directional, the $\overline{E}$ values obtained cannot be expected to be the true $\overline{E}$ values. However, comparisons among $\overline{E}$ values taken at different locations or with different Bevatron conditions have proved quite useful. A few examples will illustrate this point.

A number of $\overline{E}$ measurements were made during the mezzanine surveys of late 1956. (The face of the Hansen-McKibben counter was covered with 0.030 inch Cd during these runs.) The counters were stationed at the front of the mezzanine at the center of Bay 20, that is, nearly midway along the

southwest magnet quadrant, and at an elevation of 17 ft above the main floor. Values for $\overline{E}$ of 0.4 Mev were obtained with the southwest shield at its normal height, 19 ft. Values for $\overline{E}$ rose to 0.5 Mev when the top 4 ft was removed from this shield. Polyethylene counter data showed 31 Mev/cm^2 per 10^{10} protons and 48 Mev/cm^2 per 10^{10} protons, respectively, for these two shield conditions. Removal of the shield material is seen to cause a significant increase in the energy flux density reaching the counter. The corresponding rise of the $\overline{E}$ value shows that this increase represents a shift toward higher energy in the neutron spectrum rather than just an increase in total incident flux.

Several $\overline{E}$ determinations were made at the Bay-20 station with the Hansen-McKibben counter covered by a $1\frac{1}{2}$-inch-thick slab of paraffin in addition to the Cd sheet. (This filter attenuates Sb-Be neutrons by a factor of 5 and so is assigned an energy cutoff of 30 kev.) The $\overline{E}$ values ranged between 1.8 and 2.0 Mev, showing that there exists a considerable high-energy component. It is thought that most of these higher energy neutrons (> 1 Mev) reach the mezzanine by air scattering over the shield rather than by penetration of the shield or by generation within the shield itself.

It is difficult to relate the $\overline{E}$ values so obtained to the biological hazard associated with this neutron flux. If the maximum permissible flux were independent of neutron energy, then $\overline{E}$ values could be used directly to evaluate the hazard. However this condition is not fulfilled for the energy range containing all but a small fraction of the total neutron population (below 5 Mev). Thus hazard evaluations based on $\overline{E}$ will generally be incorrect and will be overestimates, depending on neutron spectral distribution.

Other Methods

Other methods employed to investigate the distribution of neutron energies behind the shield have included visual observation of a diffusion cloud chamber and scanning of proton-recoil tracks in Eastman Kodak NTA film. The cloud chamber shows many more short and fewer long proton recoil tracks than are produced by a Po-Be neutron source. The emulsion tracks show similar characteristics relative to Po-Be induced events. Stars are rarely observed in the emulsions, indicating that few very-high-energy neutrons are present. Both detectors point to the same conclusion—that Bevatron stray neutrons carry considerably less energy per neutron than do Po-Be neutrons. This is in accord with all other information.

The use of a system of threshold detectors is expected to provide more detailed and more precise information regarding the neutron-energy distribution. It has been shown that such a system is useful for neutron intensities down to the vicinity of maximum permissible flux levels.[6] A program is in progress to investigate the feasibility of such detectors for survey work in occupied areas, with particular emphasis placed on pushing downward the lower limits of detectable flux. For example, it looks quite reasonable to detect the activation produced in the C^{12} (n, 2n)C^{11} reaction from a flux of 1 n/cm^2-sec above the 20-Mev threshold. Among the other elements being considered are thorium, U^{238}, sulfur, iron, nickel, and bismuth. Major problems with these detectors include reduction of

background-radiation count rates to a minimum, and development of methods to incorporate large amounts of active material into high-efficiency counting systems.

Neutron-Energy Determination: Summary

The results obtained from these methods are approximate and can often be interpreted only in a qualitative manner. It is reasonable to expect that more quantitative information can be obtained from both the paraffin buildup and the Hansen-McKibbon-PE counter systems as the properties of these systems become more completely understood. Certainly the threshold detectors can provide quantitative data within their respective minimum-detectable-flux requirements. Unfortunately the threshold energies available are fixed by nuclear properties of the elements, and are not spaced ideally for detailed examination of neutron spectra.

Details of the neutron spectra may be revealed when the neutron spectrometers now under development become operational. The two instruments that now show the greatest promise are both 4-pi detectors and should complement each other in energy response. The first, based on the He^3 (N, p)H^3 reaction will cover the energy range from 0.05 to ~1.0 Mev. The second device, a two-counter total-absorption proton-recoil detector, is expected to be useful from 3 to 4 Mev upwards,[7] and may provide coherent data from even lower neutron energies, thus narrowing the gap between the respective response ranges.

NTA FILM MEASUREMENTS

Bevatron personnel is provided with fast-neutron-sensitive film as a part of the UCRL film-badge program. Readings from these films have in general agreed with counter measurements, insofar as comparisons have been possible. Film readings have increased steadily with increasing beam magnitude; readings from personnel who spend most of the time at mezzanine level are higher than readings from main-floor occupants. These are general trends, observed only over a long period of time.

The NTA films have also been used in survey work to determine fast-neutron flux levels at various locations around the Bevatron. The most extensive coverage of the building was obtained from three sets of films exposed in November and December 1955 during a period of steady high-intensity beam and constant experimental conditions. Each set included 41 films; successive sets repeated the first-run locations.

Film characteristics and handling techniques are as follows. Eastman Kodak NTA film has an emulsion 25 μ thick which is approximately the same sensitivity as Ilford C-2. After development, films are examined with a Bausch and Lomb Model TPR-1 microscope using a 43X (high, dry) objective and 10X eyepieces. An eyepiece reticle limits the field of view to a square 245 μ on a side. Tracks are counted until either 100 fields are examined or 100 tracks are observed.

Calibrations of film are performed in the known fluxes from neutron sources. After the film is exposed to 4.32×10^6 n/cm^2, from a Po-Be source 1.5 tracks per field are developed; 0.77 tracks per field are developed from an exposure to 4.32×10^6 n/cm^2 from a mock-fission source. The developed background is approximately 0.08 tracks per field. This number has been subtracted from the data of Fig. 29.

Figure 29 shows the results of these exposures for the most important locations; the average of three values is reported in terms of tracks per field per 10^{14} protons of 6.2-Bev energy. The number of protons per exposure was determined by the central monitor counter. The encircled numbers on Fig. 29 are energy flux-density levels measured with the PE-lined counter; these are listed at locations near film positions for comparison purposes.

The acceleration of 10^{14} protons to 6.2 Bev required something like half a week at the time of these exposures; thus if track-per-field values are multiplied by 2, a reasonable approximation to a weekly exposure is obtained. It is difficult to make direct comparison between film data and PE counter data, since film sensitivity drops sharply for neutrons below 1 Mev energy. Thus the film is insensitive to an energy range containing a large neutron population. Until more details of the spectrum are learned, it is not clear how to correct the two kinds of data so that quantitative agreement can be expected. Inspection of Fig. 29 shows however that film and PE data generally follow the same pattern.

Another film study, conducted during the same period, showed the vertical pattern of fast-neutron flux at the junction of Bays 19 and 20 just in front of the mezzanine wall. Films were arranged at 5-ft intervals from floor level to 30 ft in elevation, and exposed for a period of one week. Figure 30 shows the distribution obtained by this method. The flux is seen to increase with elevation, showing a rise of a factor of nearly 2 between floor and mezzanine levels (agreement with PE-counter data) and a further sharp rise at the greatest height investigated. This increase is to be expected, because air scattering over the shield will produce this sort of effect for elevations below the shield top, and a more unobstructed view of the machine will produce a further rise in flux as height is gained above the shield top.

FOIL-ACTIVATION TECHNIQUE

Indium-foil activation has been employed extensively in the measurement of fast-neutron flux levels since December 1956. The method consists of irradiation of the foils placed inside 6-inch-diam. paraffin spheres, with the spheres in turn surrounded by 0.030-inch cadmium shields. After irradiation at the selected locations, the 54-min activity induced in the foils is followed for at least one half life with Geiger-Mueller tube–scaler counting equipment. Extrapolation of the activity curves back to the time the exposure ended then gives the activity induced in each foil to this time and thus permits simultaneous comparison of neutron-flux levels.

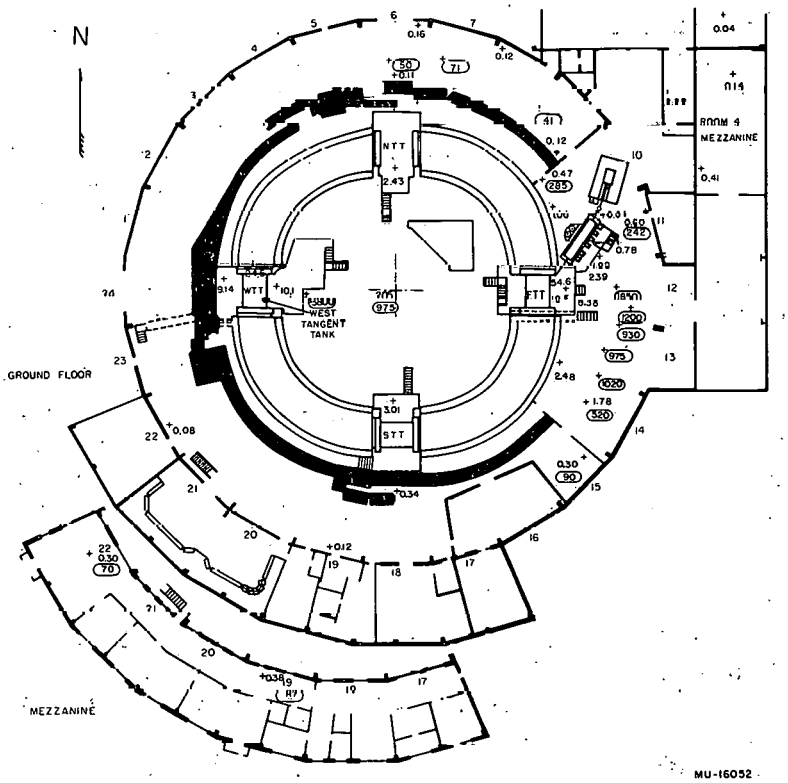

Fig. 29. Eastman NTA film study of Bevatron fast-neutron field: complete building survey, showing tracks per field per 10^{10} protons at 6.2 Bev. Encircled values are measurements made with PE-lined counter in Mev/cm^2/10^{10} protons at 6.2 Bev.

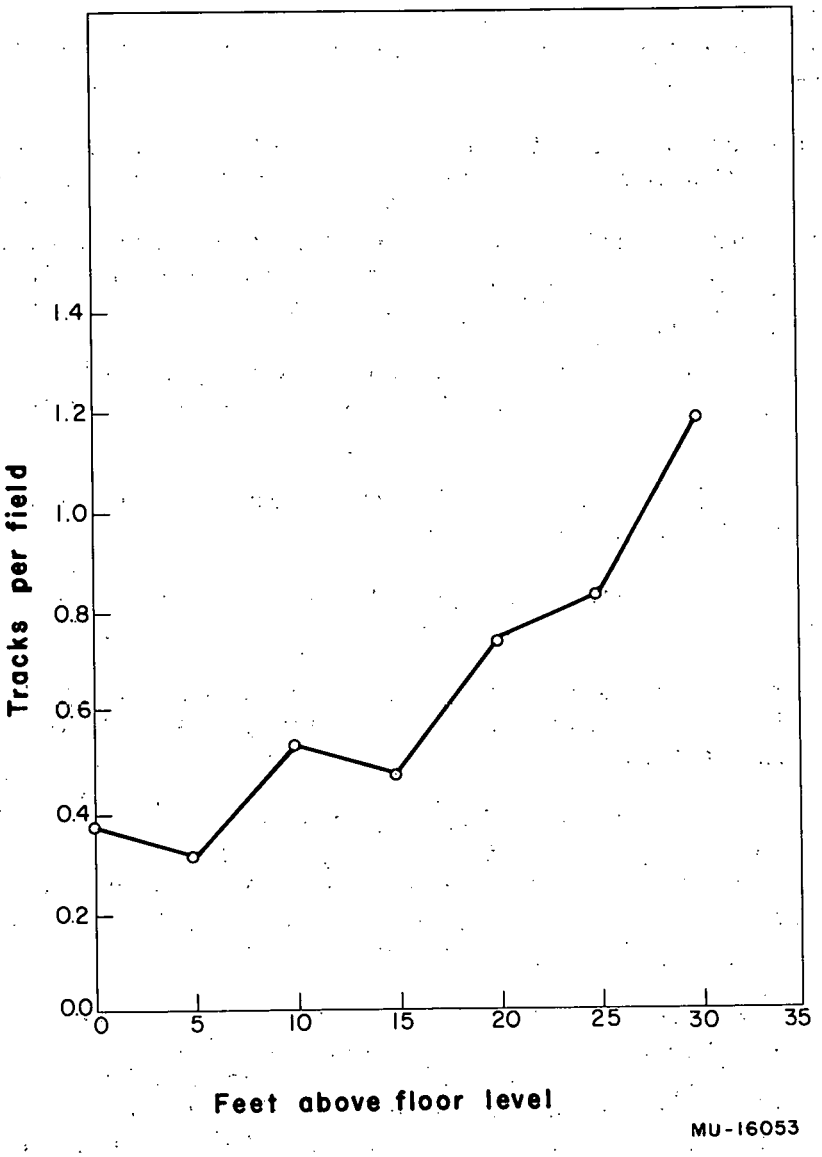

Fig. 30. NTA film study of Bevatron fast-neutron field; elevation survey, Bays 19 and 20.

This technique offers several important advantages for survey work at the Bevatron:

(a) Simultaneous measurements can easily be performed at the different locations.

(b) The number of simultaneous measurements is essentially unlimited; likewise, the choice of survey locations is unrestricted.

(c) Results are unambiguous, as only neutrons can induce the detected activity; there are no problems of discrimination against gamma flux, as with proportional counters.

(d) Counting rate problems are nonexistent; thus foils can be used in radiation fields so intense that counters would be completely useless.

(e) The method is extremely simple in practice, and yields results in a delightfully short time.

There are also several disadvantages to the use of indium foils for this sort of measurements:

(a) The method is energy-insensitive as employed to date; measurements do not give results directly interpretable in terms of biological hazard.

(b) The relatively short half life for the induced activity, 54 min, precludes use of these foils to integrate the neutron flux. On the other hand, the somewhat erratic operation of the Bevatron mitigates against irradiation to saturated activity. Thus absolute quantitative information is difficult to obtain.

(c) The activation induced by neutron fluxes of tolerance level yields a low counting rate with present equipment. The system in use produces 35 c/m per gram of indium irradiated to saturation in a flux of 30 n/cm^2 sec Po-Be neutrons, or 80 c/m from a typical foil. The background level for the counter is 20 c/m. Both increased sensitivity and decreased background are required from the counting system for this technique to be reliable at lower flux levels.

Foil-activation measurements have been most useful in studies of the neutron-flux distribution inside the magnet ring. At these locations it is of paramount importance that comparative measurements be taken simultaneously. In addition, the instantaneous counting rates encountered here would paralyze the electronic equipment used with proportional counters.

Data obtained from three series of foil measurements are shown in Figs. 31, 32, and 33. A set of 16 foils was arranged along the inside of the magnet structure. Those at tangent tanks were placed on the platforms at

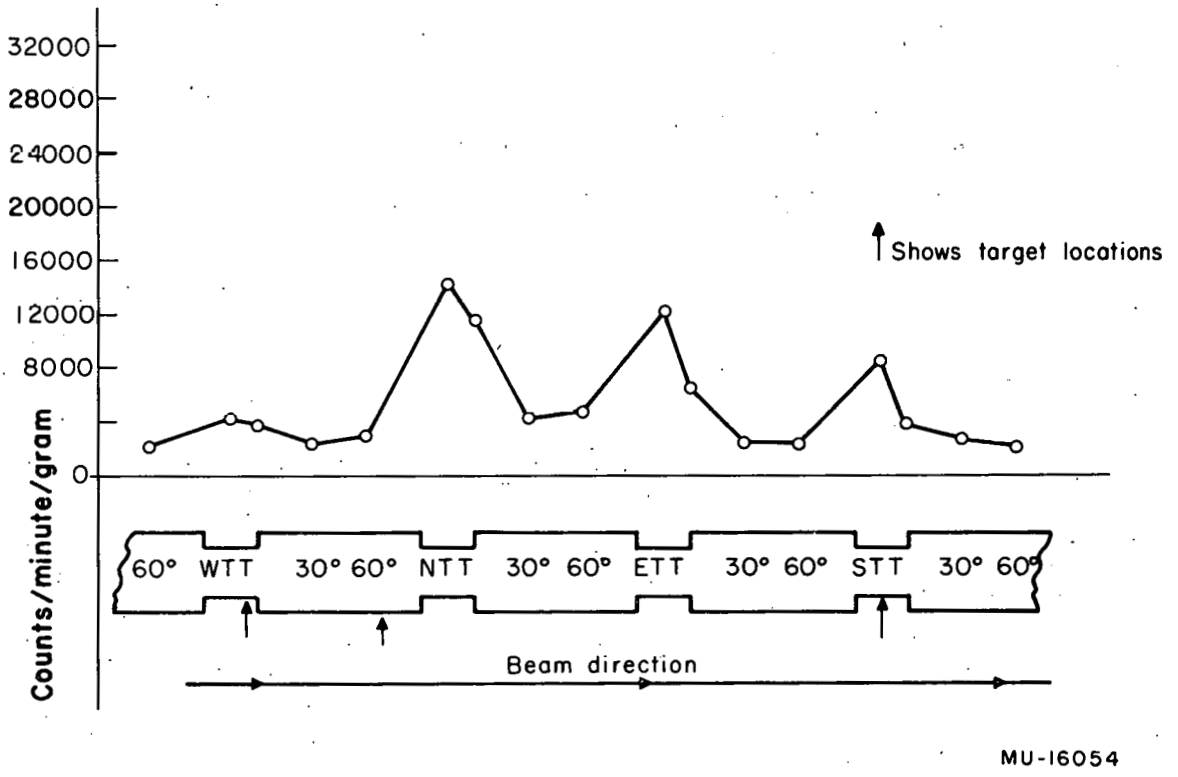

Fig. 31. Indium foil run 1; fast-neutron flux inside the magnet ring. Actual monitor-foil activity; 1850 counts/minute/gram. Beam is $\sim 3 \times 10^{10}$ 6.2-Bev protons/pulse.

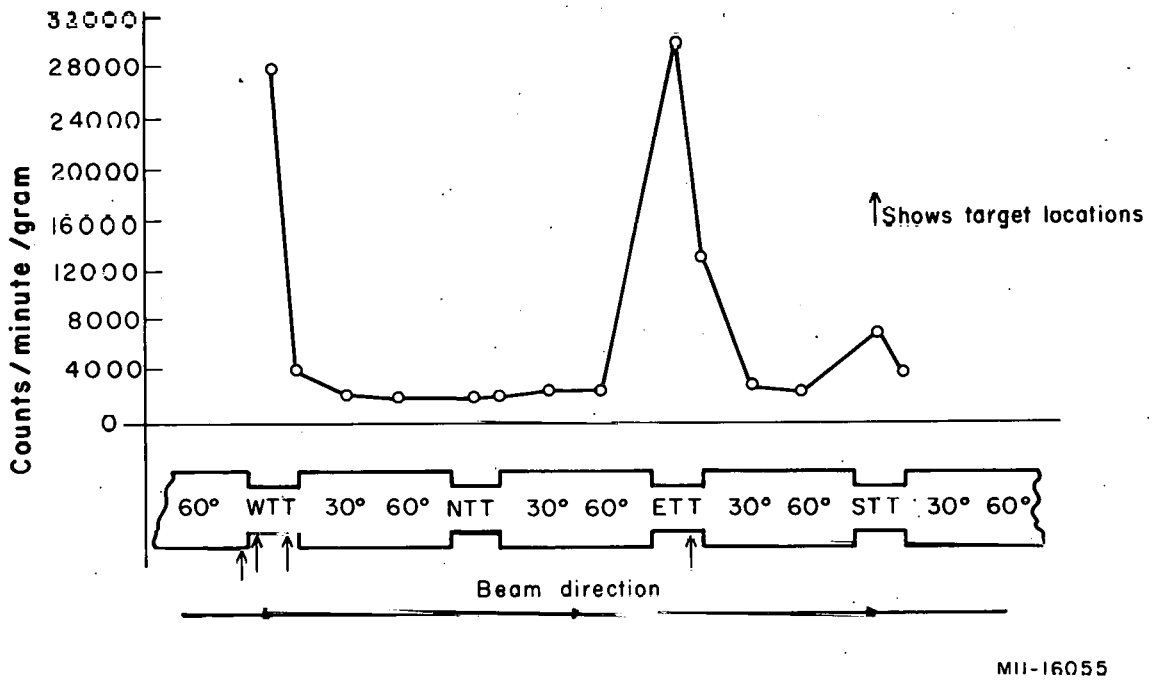

Fig. 32. Indium foil run 2; fast-neutron flux inside the magnet ring. Actual monitor-foil activity: 1850 counts/minute/gram. Beam is $\sim 5 \times 10^{10}$ 6.2-Bev protons/pulse.

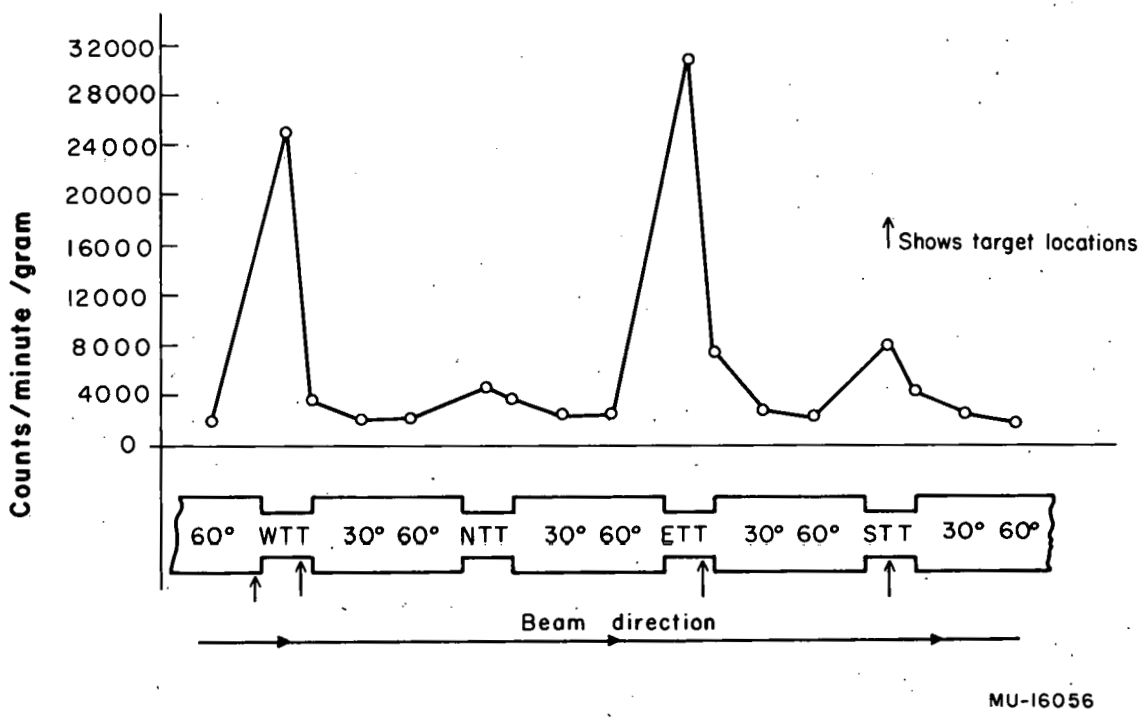

Fig. 33. Indium foil run 3; fast-neutron flux inside the magnet ring. Actual monitor-foil activity: 4480 counts/minute/gram. Beam is $\sim 6 \times 10^{10}$ 6.2-Bev protons/pulse.

the center and downstream edge, respectively. Those at magnet quadrants were placed on the walkway at 30° and 60° points. All foils were nearly equidistant from the center of the pit, and close to the median plane of the beam. An additional foil, located at the central monitor position in the pit, serves as a monitor for comparison of the three runs. Thus, Figures 31, 32, and 33 show response of the 16 foils normalized to 1850 c/m per gram of indium from the monitor foil. Sharp peaks are seen at the tangent tanks, and a relatively uniform low level exists along the magnet quadrants. The relative peak intensities change understandably with different target situations.

A detailed examination of Bevatron operating conditions for each set of exposures clarifies this pattern, and explains the few apparent inconsistencies in the above picture. Table VI presents this information and also includes notes and comments pertinent to the respective runs.

It is evident that the major neutron-yielding areas are the tangent tanks, and then only when a nearby target or other obstruction is presented to the accelerated beam. Disappearance of the NTT peak when the nearby target was not used (runs 2 and 3) shows this effect clearly. Further confirmation is offered by the great elevation of the ETT peak noted when the plunging clipper operated (again Runs 2 and 3). The low levels seen along magnet quadrants also lend support to the pattern as described above. It is interesting to note that if one assumes that all the neutron flux emanates from tangent tanks, the expected level at the central monitor station is nearly the observed value.

The radial pattern of the thermal-neutron flux was investigated with bare indium foils at this time for an azimuth through Bay 20. Foils were suspended on a cable at an elevation of 20 ft above floor level. A section view of the Bevatron showing locations of the foils appears in Fig. 34. Two separate foil exposures were taken., Points 1 to 9 inclusive and points 9 to 17 inclusive. Bevatron operating conditions remained constant for both runs. Data was normalized to Location 9, and a plot of results is shown as the upper curve on Fig. 35. The slow flux at this azimuth is relatively constant in the magnet pit, is somewhat depressed over the magnet structure, drops significantly as the shield wall is passed, and then decreases slowly with increasing radial distance.

The lower curve on Fig. 35 shows a relative plot of results obtained at the same elevation and azimuth with foils in paraffin enclosed in Cd boxes. The fast-neutron flux as seen by this detection system does not show a significant drop as the shield is passed, but rather exhibits a very gradual decrease with distance from the pit center.

These profiles are probably characteristic for regions along the machine well away from any localized neutron-producing area. Profiles taken at or near a tangent tank containing an active target would look quite different, and would show peaks in both fast and slow fluxes close to the machine.

Foil data has provided the first coherent picture of neutron-flux distribution inside the magnet ring. Previous data obtained with other types of

Table VI

Bevatron conditions for indium foil runs[a]

Run No.	Date	Targets				Beam conditions		
		Location	Material	Thickness (inches)	Arrival I pip	Energy (Bev)	Intensity (protons/pulse)	Pulse rate (Pulses/minutes)
1[b]	1/15/57	WIN	Mylar aluminum	0.016 0.001	I_{30}	6.2	$\sim 3 \times 10^{10}$	10
		69°D[c]	aluminum		I_{30}	6.2	$\sim 3 \times 10^{10}$	10
		SOW	aluminum	0.00025	I_{30}	6.2	$\sim 3 \times 10^{10}$	10
2[d]	1/16/57	WIN	polyethylene	0.5	I_{29}	6.2	$\sim 5 \times 10^{10}$	10
		WIS	copper	1	I_{25}	6.2	$\sim 5 \times 10^{10}$	10
		1°59"U[c]	copper	1	I_{27}	6.2	$\sim 5 \times 10^{10}$	10
		EIS	copper	6	I_{29}	6.2	$\sim 5 \times 10^{10}$	10
3[e]	1/30/57	WIN	carbon	0.5	I_{29}	6.2	6 to 8×10^{10}	10
		1°59"U[c]	carbon	1	I_{27}	6.2	6 to 8×10^{10}	10
		SOW	aluminum	0.00025	I_{30}	6.2	6 to 8×10^{10}	10
		EIS	copper	6	I_{29}	6.2	6 to 8×10^{10}	10

[a]No activation times listed for runs, because machine operation usually renders this sort of information misleading. All foils normalized in respect to foil at center of magnet pit.

[b]Comments: (1) WTT–center foil behind concrete shield block; peak obscurred; (2) NTT–peak produced by 69° target; (3)ETT–peak probably related to injector apparatus in tank; (4) STT–peak probably related to SOW spillout-control foil and induction-electrode system in tank; and (5) magnet quadrants–low uniform levels.

[c]Angular positions of targets measured from WTT; U indicates upstream, and D indicates downstream.

[d]Comments: (1) WTT–center foil inclear; peak very pronounced; (2) NTT–peak absent; no nearby target; (3) ETT–peak much higher than for Run 1 and associated with clipper located here; (4) STT–peak similar to that for Run 1; (5) magnet quadrants–low uniform levels; and (6) no date from two foils in SW magnet quadrant.

Table VI (contd)

[e]Comments: (1) WTT–peak as for Run 2; (2) NTT–peak essentially absent; (3) ETT–peak as for Run 2; (4) STT– peak as for Run 1; (5) Magnet quadrants – low uniform levels; and (6) this profile very similar to that for Run 2.

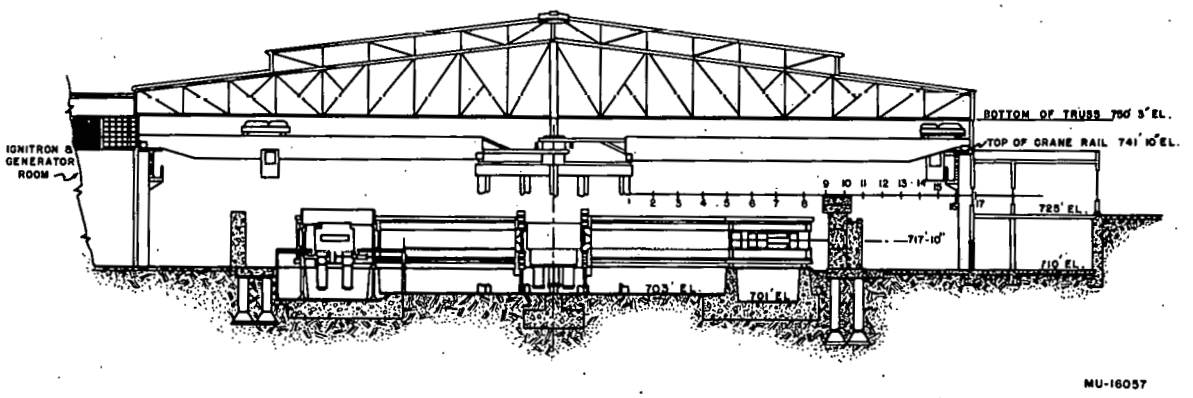

Fig. 34. Section view of Bevatron at Bay 20.

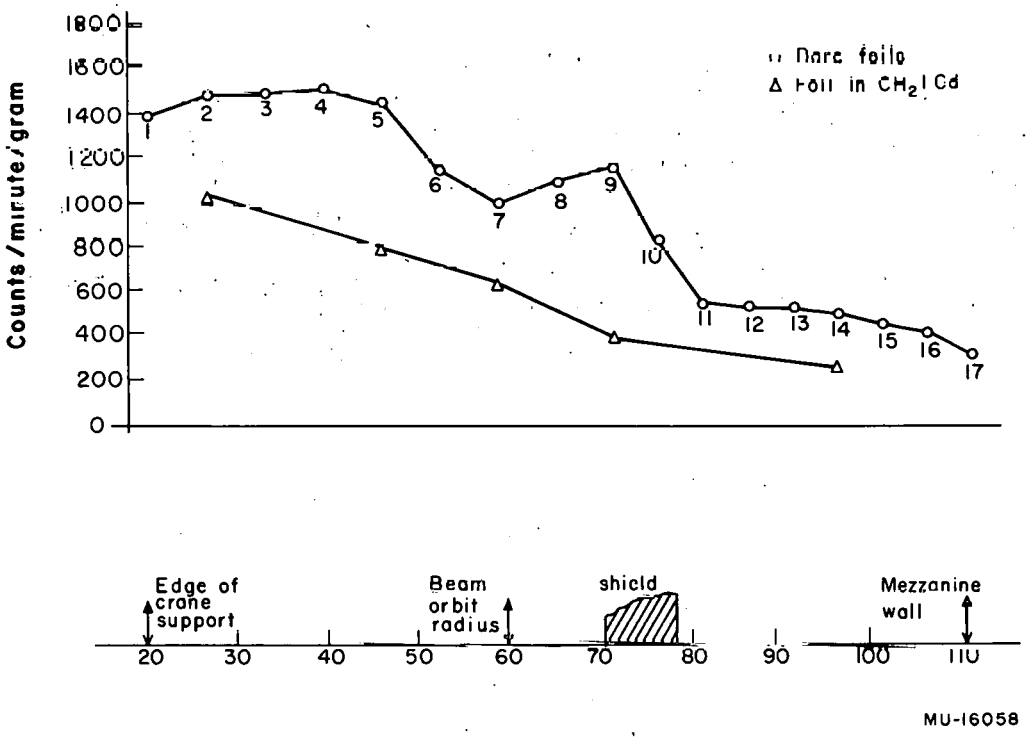

Fig. 35. Indium foil study of neutron flux along a radius at Bay 20. Beam is 2 to 3 × 10^{10} protons/pulse at 6.2 Bev with 3° carbon target at I_{29}.

detectors have yielded only fragmentary glimpses of the role played by various segments of the machine as neutron sources. Moreover, none of this information revealed the apparent sharp delineations of the neutron-producing areas indicated by foil measurements. It is expected that the understanding gained through these experiments will enter significantly into shield considerations for the future.

TECHNIQUES FOR RAPID SURVEYS

Situations arise in which the hazard existing at some previously unsurveyed location must be determined quickly. Such situations usually result from experimental conditions that require changes in shielding and access to areas not normally open to personnel. The portable integrating electrometer and plastic-wall ion chambers are used for these surveys. An RBE (relative biological effectiveness) value of 10 is assigned to the response of the instrument when readings are interpreted in terms of biological hazard. As an additional check, a measurement is taken at a nearby location that should be unaffected by the special conditions and at which the radiation level is known from previous measurements. Experience has shown that this sort of quick surveying technique is satisfactory in most cases; for the few remaining situations, standard survey equipment is brought into operation and three-component measurements are taken.

SUMMARY

The various radiation detectors described in the foregoing pages have been employed to measure the stray radiation field of the Bevatron. These measurements have made it possible to construct a general pattern for each of the three significant components of the field: the fast-neutron, slow-neutron, and gamma-ray fluxes.

As a biological hazard, the fast-neutron component is the most important; thus greatest emphasis has been placed on measuring and understanding the characteristics of this flux. Current evidence shows that the main shield is of adequate thickness and that air scattering over the shield top contributes a significant amount to the fast-neutron flux seen outside the shield. It is undoubtedly true that the apparent effectiveness of the relatively thin main shield is, to a considerable extent, due to the presence of a 2-ft-thick iron flux-return path along the outer periphery of the magnet at the median plane. The tangent tanks are revealed as major areas for neutron emission from the accelerator, especially if obstructions or targets are presented to the beam near these locations

Targets are almost always "thin" for protons of the energy range produced by the Bevatron; furthermore, only a small fraction of the total beam particles undergo nuclear reactions in the target material. Thus the main effect of a target on the beam particles is to degrade their energy slightly, a process that forces them to spiral inward and ultimately strike the surface of the vacuum tank. The high-energy protons will then produce secondary particles – many of them neutrons – as they are degraded in energy in passage through the magnet structure.

The shielding is rather easily arranged to contain the high-energy particles in the forward direction from targets, because the characteristics of these "beams" are well known, and the required shield area is not great. However, these beams contribute only a minor component to the total stray-radiation flux produced by the machine. The greatest source of stray radiation undoubtedly derives from the degradation in energy of the large fraction of beam that is merely deflected by the target and impinges on the vacuum-tank walls to penetrate or even pass through the magnet structure. Neutrons produced by these processes (the evaporation neutrons) may be distributed widely around the magnet ring; in addition, there are no directional properties associated with this sort of neutron emission. It is therefore evident that shielding against these neutrons cannot be done simply and economically, as for beam particles, but must essentially require shielding the entire accelerator. It should be mentioned that a significant gain in shield effectiveness may be brought about through the addition of shield material around the open sides of tangent tanks. However, these areas are vital to operational and experimental purposes and cannot be indiscriminately buried in massive shielding. These are the major problems to be considered as the Bevatron becomes a more dependable machine, capable of producing high-energy proton beams of increasing intensity. Beam levels of 5×10^{10} ppp are a reality; beam levels of 2 to 3×10^{11} ppp will probably be achieved in the near future. The radiation levels likely to accompany this higher beam intensity must then be assumed to exist, and as a minimum objective means must be found to keep these levels within the safe limits currently prescribed.

The course for much of the future Health Physics work at the Bevatron has already been described under respective section headings. The general areas in which efforts will be concentrated are, further determination of characteristics of the radiation field, determination of the neutron energy spectrum and identification of the roles played by various parts of the accelerator in neutron production. Information gained from these investigations is immediately useful to evaluate the biological hazard; it is also important data for shielding calculations. The purpose is twofold: to extend and clarify the understanding of the radiation field, and to provide information that indicates methods to reduce further the radiation levels in occupied areas.

ACKNOWLEDGMENTS

The work reported here has involved the entire staff of the Health Physics Group in varying degrees. Of special importance are the contributions of Dr. Burton J. Moyer, Dr. Roger W. Wallace, H. Wade Patterson, Joseph B. McCaslin, Lloyd D. Stephens, and Theodore M. Jenkins. A partial list of their contributions includes: assistance in actual radiation-survey work, assistance in data interpretation, development of counting techniques, and critical comment on this report during its preparation.

The cooperation of the Bevatron staff during certain phases of this work was appreciated.

This work was performed under the auspices of the U. S. Atomic Energy Commission.

REFERENCES

1. Edward J. Lofgren, The Bevatron and Its Place in Nuclear Physics, UCRL-3372, April 6, 1956.

2. William M. Brobeck, Design and Construction of the Bevatron, UCRL-3912, Sept. 13, 1957.

3. A. O. Hanson and J. L. McKibbon, Phys. Rev. 72, 673 (1947).

4. Nobles, Day, Henkel, Jarvis, Kutarnia, McKibbon, Perry, and Smith, Rev. Sci Instr. 25-4, 334 (1954).

5. Burton J. Moyer, Survey Methods for Neutron Fields, UCRL-1635, Jan. 11, 1952, Nucleonics 10-5, 14 (1952).

6. Hurst, Harter, Hensley, Mills, Slater, and Reinhardt, Rev. Sci. Inst. 27 No. 3, 153 (1956).

7. John W. McCord, A Double-Pulse, Total-Absorption Spectrometer for Neutrons (Thesis), UCRL-3411, May 11, 1956.

Information Division
br